Automatic Breath Phase Detection using only Tracheal Breath Sounds

by

Saiful Huq

A Thesis submitted to the Faculty of Graduate Studies of

The University of Manitoba

in partial fulfillment of requirements of the degree of

MASTER OF SCIENCE

Department of Electrical and Computer Engineering

Faculty of Engineering

University of Manitoba

Winnipeg

# ACKNOWLEDGEMENTS

**Dedicated to:**

*My Family*

*"Each today, well-lived, makes yesterday a dream of happiness and each tomorrow a vision of hope. Look, therefore, to this one day, for it and it alone is life"*

# ABSTRACT

Current flow estimation methods use tracheal sounds in all except one step of the process: 'breath phase detection', is done by assuming alternating breath phases or using a second acoustic channel. The alternating assumption is unreliable in long recordings; non-breathing events (apnea, swallow or cough) change the alternating pattern. Although phases can be detected using lung sounds intensity, the additional channel and associated labor is clinically impractical.

We present a method using breath sound parameters to differentiate between the two respiratory phases. The novel method is independent of flow level, requiring only one prior- and one post- breath segment to identify the phase. This was tested on data from 93 healthy individuals, without any history of pulmonary diseases, at 4 different flow levels. The most prominent features were duration, volume and shape of the sound envelope. This method showed accuracy of 95.6%, 95.5% sensitivity and 95.6% specificity.

# TABLE OF CONTENTS

# LIST OF FIGURES

# LIST OF TABLES

# LIST OF EQUATIONS

# CHAPTER I

# INTRODUCTION

Analysis of digitized breathing sounds opens the avenue to objective diagnosis as opposed to the subjective assessment by a healthcare professional's stethoscope. Identifying key variables from breath sounds provides further information about the respiratory system, adding to the standardizing toolset available to aid healthcare professionals and respiratory specialists.

The stethoscope has evolved over nearly 200 years and still remains an essential tool for physicians and doctors. Nevertheless, stethoscopes provide a very subjective assessment of the respiratory system. It is largely agreed upon that near the late 1950's was the beginning of objectively viewing respiration by time-frequency analysis [1]. Since then, respiratory sound analysis has become increasingly sophisticated in terms of data-capture, analysis and implications of respiratory sounds mainly in assessment of the health of an individual's respiratory system [2-5].

Respiration is an essential metabolic process necessary for human beings for the production of energy using oxygen from the air and glucose from consumed food [6]. Many diseases and disorders have been shown to stem from the improper functioning of this fundamental process [7]. Thus, being able to monitor the proper functioning of this system will greatly benefit the general wellbeing of an individual.

## 1.1   Motivation

Current breathing flow estimation methods rely heavily on tracheal breath sounds. One major step of the process however, 'breath phase (inspiration/expiration) identification', is done by either assuming alternating breath phases or using a second acoustic channel of lung sounds [8, 9]. The alternating assumption is unreliable since in long recordings, non-breathing events such as apnea, swallow or cough change the alternating nature of the phases [**10**]. Although breath phase can be easily detected using lung sounds intensity, this requires the addition of a secondary channel and the associated labor. Hence, an automatic and accurate method for breath phase detection using only tracheal sounds would be of great benefit.

## 1.2   Goals and Objectives

The purpose of this thesis is to contribute to current breathing flow estimation methods by providing a novel approach to breath phase identification. The specific objectives of the thesis are:

- Developing experimental protocols for the analysis of respiratory sounds with a focus on phase detection.
- Develop a tracheal breath sound dataset that adheres to strict experimental protocol to obtain a representative sample of the general healthy adult population.
- Determine key features of the breath sounds that assist in phase detection.
- Determine the anthropomorphic effects on the extracted key features.

- Develop a phase detection method that is simple, using only one channel of breath sounds (tracheal), does not rely on calibration, and is robust across different flow levels.

## 1.3   Organization of Report

The manuscript is structured into five chapters. The first chapter introduces the reader to the motivation, goals and objectives of the thesis. This is followed by literature review and background in the second chapter. This focuses mainly on the respiratory system and its intricacies and functionality of the different mechanical aspects of the system. It also gives a background on the neurological system that controls respiration, and notes the different methods used to date for monitoring of respiration. Chapter three describes in detail the methodology adopted for this project. This includes the experimental setup, the screening process for healthy participants, as well as the protocol followed for the experiment. Chapter four presents the results and discussion portions of the report. The final chapter presents concluding remarks on the project completed and suggests future paths to take for the continuation of this study.

# CHAPTER II

# LITERATURE REVIEW AND BACKGROUND

## 2.1   The Respiratory System

Respiration can be divided into internal and external respiration. Internal respiration is the method by which oxygen and carbon dioxide is carried between the lungs and the body organs, while external respiration refers to the movement of air from the external environment to the lungs [11]. We will refer to external respiration when we use the term respiration.

A complete respiratory cycle involves the movement of air from the environment into the lungs (inspiration) followed by the expulsion of the air into the environment (expiration). In a healthy adult at rest, a respiratory cycle would result in air exchange at the rate of 4 liters/minute [11]. In order to absorb the required amount of oxygen into the body, the cardiac system would require pumping about 5 liters/minute of blood through the pulmonary vessels for internal respiration. This ratio is very sensitive to activity and oxygen demand.

## 2.2   The Structures

During inspiration, air passes through the nostrils and nasal cavity (air can also enter through the mouth and oral cavity), into the pharynx, past the larynx and trachea (Figure 1) and goes into the lungs as the trachea bifurcate into the bronchi and continue to bifurcate into smaller airways [1, 6]. In an adult, these bifurcations continue for about 23

generations. With each bifurcation, the airway diameter becomes smaller, its length becomes shorter and the walls become thinner. Internal respiration begins at around the 17th generation of the airway bifurcations as alveoli start appearing. This is the beginning of the respiratory zone, while everything above this portion is considered the conducting zone [**12**]. The details of both these zones will be explained in some detail in the following sections.

### 2.2.1  Conducting Zone

The nasal cavity has a mucosal lining throughout, except for the vestibule, which is lined with skin. This skin has vibrissae (hair) that prevent any large particles from entering the nasal cavity [**13**]. There are 3 distinct structures within this cavity called conchae that separate the area into 4 passageways. This allows for a greater surface area and more air turbulence. Deep to the nasal mucosa lies a rich plexus of veins that provide thermoregulation; The large surface area and plexus of veins warms and moistens the air during inspiration and cools and reabsorbs moisture from it during expiration to efficiently utilize body heat and water. Four sinuses that also help in thermoregulation surround the nasal cavity. Along with olfactory (smell) sensory nerves, the nasal cavity has various sensory nerve endings as well. These nerves detect the presence of irritants and large foreign particles that trigger a sneeze reflex to expel the particle from the respiratory system.

Air can also enter the lungs through the oral cavity, though the nasal passage is used most often. The posterior end of both cavities open into the pharynx, which further separates inferiorly to the esophagus and the larynx. The esophagus is normally collapsed and the larynx is open [13, 14]. Superiorly, the larynx connects to the hyoid bone and

inferiorly it opens to the trachea. By an intricate sequence of maneuvers, known as the swallowing mechanism, the epiglottis closes the larynx and opens the esophagus to allow food and fluids into the stomach. Vocal cords are housed in the larynx, and speech sounds are produced when these cords come together and vibrate as air passes over them. During regular breathing, the vocal cords and epiglottis are open and allow the air to pass through to the trachea.
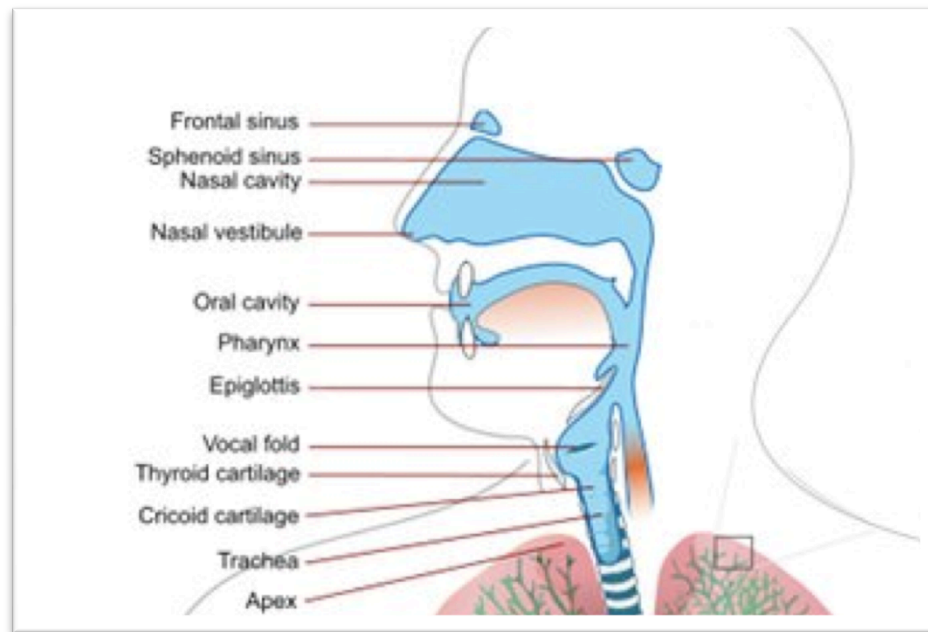


**Figure 1. Head/Neck portion of the respiratory system [15]**

The trachea and bronchi are held open with the support of C-shaped hyaline cartilage rings [**13**]. The openings of the rings are on the posterior wall of the trachea, and are connected by a smooth muscle called the trachealis. This muscle allows the esophagus to expand as bolus travels through it, without causing damage to the trachea. Deep to the pseudostratified, ciliated epithelium layer, the tracheal walls have various elastic fiber enriched layers among the fluid secreting glands. These layers along with the C-shaped cartilaginous rings keep the airway open while allowing the neck full range of

motion. The contraction of the trachealis smooth muscle reduces the cross-sectional area of the trachea, increasing the internal pressure [**16**]. During coughing, this action helps expel mucus from the trachea.

Except for the oral cavity and the oropharynx, the conducting zone is lined with a very unique epithelium layer (Figure 2). The cells are pseudostratified, ciliated cells and have two layers of fluid on top. These fluids are part of the defense mechanism and are constantly replenished by glands and special cells (goblet) within and below the epithelium layer. A sticky mucus layer captures any dust particles and foreign objects that get past the nasal vibrissae (long hair-follicles at the nasal opening). Deep to the mucus layer is a more watery fluid. This fluid contains enzymes that break down unwanted bacterial matter and also keep the cilia lubricated and prevent them from sticking to the mucus layer [12, 13]. The cilia are specialized hair-like structures, with no muscle fibers, which constantly beat against the mucus layer causing a smooth, flowing sheet of mucus in one direction, regardless of breath phase (inspiration/expiration).
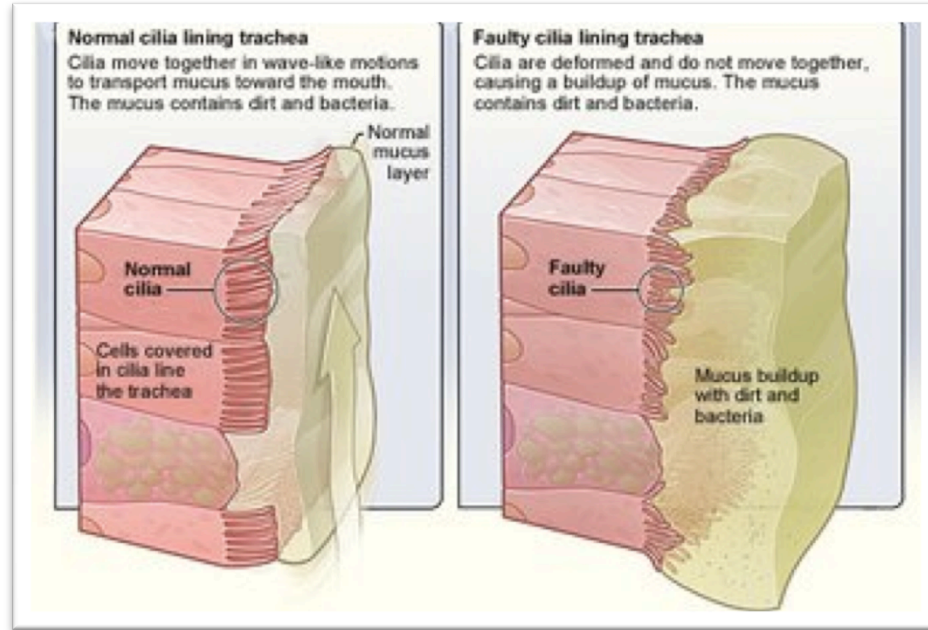
**Figure 2. Typical normal and faulty epithelium layer [17]**

From the nasal cavity, mucus layer flows downwards and from the tracheal and bronchial airways, mucus flows upwards towards the pharynx so that the foreign particles can be either expelled (through the mouth) or swallowed and digested. The control of cilia is still not fully understood, however, it is known that cold temperatures and cigarette smoke can harm the regular motion of these structures [**18**].

### 2.2.2 Respiratory Zone

The trachea bifurcates into the right and left main bronchi that enter into the right and left lungs respectively. The right lung is made up of 3 separate lobes while the left is made up of two. The right and left main bronchi separate and supply each of the 5 lobes and continue to bifurcate within them for a total of approximately 23 times. Each time, the airways become shorter and narrower giving way to the respiratory zone.

Travelling down the bifurcation tree, the airway wall structures change from the tracheal and main bronchi arrangement. The cartilaginous rings are replaced with

cartilage plates for support in bronchiole walls. The epithelium becomes thinner and cilia become sparse. In smaller airways (alveolar ducts) cartilage disappears completely, while the amount of smooth muscles increases. The ciliary defense mechanism gets replaced by microphages; structures that engulf foreign particles, preventing them from causing harm to the gas exchange sites.

The alveolar sacs are the terminal structures of the airways (Figure 3). These are clusters of bubble-like structures where gaseous exchange occurs. Each individual bubble is called an alveolus. The alveolar walls are extremely thin and are surrounded by pulmonary capillaries [19]. The interior walls of the alveoli are lined with a surfactant containing fluid. Oxygen from the air within the alveoli dissolve in this fluid and diffuse across the alveolar wall into the pulmonary capillary blood while $CO_2$ diffuses in the opposite direction and into the air within the alveoli. Continuous replacement of alveolar air and pulmonary blood controls the rate of diffusion.

Other than the heart, the thoracic cavity is completely filled by the lungs. The lung tissue is mostly elastic fibers making the lungs soft, spongy and expandable. A thin, double-layered sheath surrounds each lung and is known as the pleurae. This sheath produces pleural fluid within its 2 layers. The surface tension of the fluid makes the lungs adhere to the internal walls of the thorax while the fluid acts as a lubricant, allowing the lungs to move with the thoracic cage during respiration.
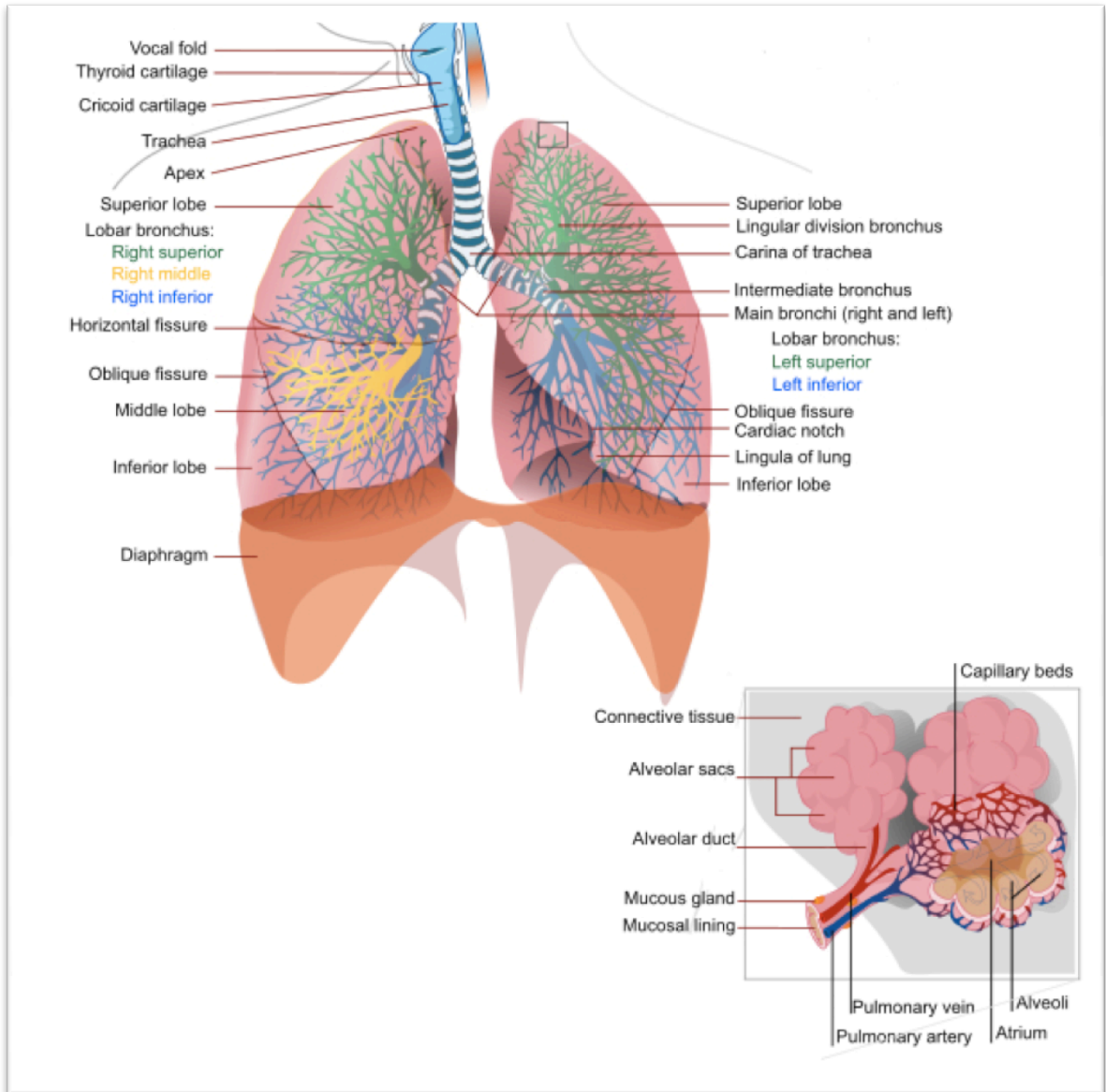
**Figure 3. Alveolar sac structure [15]**

There will always be a minimal amount of air within the respiratory system (Residual Volume - *RV*), which helps keep the airways open. During regular breathing, the volume of air breathed in a single respiratory cycle is known as Tidal Volume (*TV*). Beyond *TV*, we can force ourselves to breath more air in (Inspiratory Reserve Volume - *IRV*) or out (Expiratory Reserve Volume - *ERV*). These processes however, would

require the use of the accessory muscles for both inspiration and expiration, and would arise due to greater demand or voluntary control of the respiratory cycle.

## 2.3   Lung Mechanics

As can be seen in Figure 4, the structures of the respiratory system are housed in the head, neck and thorax regions of the body [12]. The thorax is the superior portion of the trunk between the neck and abdomen. It is made up of 12 pairs of ribs that form a cage around the thoracic cavity and protect its contents; the lungs and the heart. The ribs are curved flat bones that connect the vertebrae to the sternum. Ribs are very light, yet tough structures that attach to the sternum by costal cartilages. Typical ribs (2-9) have 2 facets on the head that allow it to connect to two adjacent vertebrae. This allows for more movement and greater change in thoracic volume. Ribs also have tubercles that join the transverse processes of the vertebrae allowing for more stability.
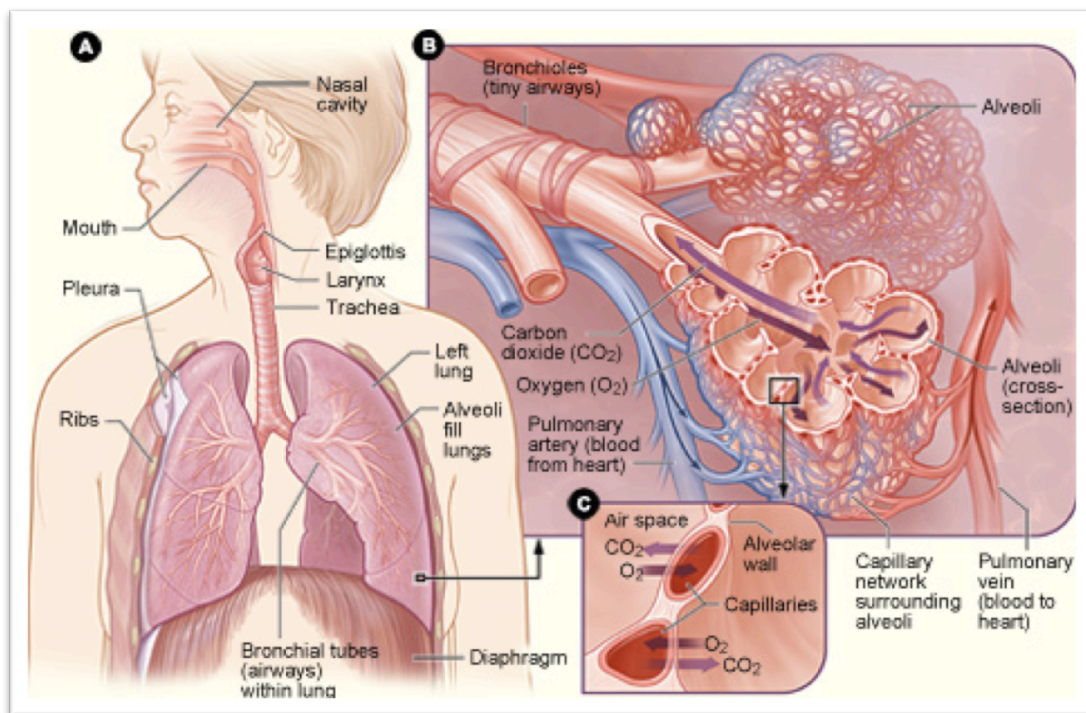


**Figure 4. Respiratory system [20]**

There are numerous muscles that surround the thoracic cavity [16]. The vital respiratory muscles are the diaphragm and the external intercostal muscles. However, since respiration is a complex process, many accessory muscles can be recruited when the breathing is stressful. These muscles are listed in the Table I. It is important to note here that in regular breathing, inspiration is an active process while expiration is a passive one [19]. However, during exercise or stressed breathing, expiration can be an active process and thus would require muscle activity.

**Table I. Respiratory muscles [21]**

| INSPIRATION | EXPIRATION |
|---|---|
| **Muscles of Trunk** | **Muscles of Trunk** |
| **Primary of Thorax**<br>Diaphragm | **Muscles of Thorax, Back and Upper Limb**<br>**Anterior**<br>Internal intercostal (interosseous portion) |
| **Accessory of Thorax**<br>**Anterior**<br>External Intercostal<br>Interchondral portion, internal intercostal<br>**Posterior**<br>Levatores costarum (brevis and longis)<br>Serratus posterior superior | Transversus thoracis<br>**Posterior**<br>Subcostal<br>Serratus posterior inferior<br>Innermost intercostal<br>Latissimus dorsi |
| **Muscles of Neck**<br>Sternocleidomastoid (superficial neck)<br>Scalenus (anterior, middle, posterior)<br>Trapezius | **Abdominal Muscles**<br>**Anterolateral**<br>Transversus Abdominis<br>Internal oblique abdominis<br>External oblique abdominis |
| **Muscles of Thorax, Back, and Upper Limb**<br>Pectoralis major<br>Pectoralis minor<br>Serratus anterior<br>Subclavius<br>Levator scapulae<br>Rhomboideus major<br>Rhomboideus minor | Rectus abdominis<br>**Posterior**<br>Quadratus lumborum |

The inverse proportionality of pressure and volume, as defined by Boyle's Law [6, 22, 23] allows air to enter and exit the lungs. When inspiratory muscles contract, the ribcage rises, increasing the thoracic cavity volume and reducing its pressure below atmospheric pressure. This forces air into the lungs (inspiration), down the pressure gradient. During regular breathing, when these inspiratory muscles relax, the ribcage presses down on the lungs and the natural elasticity of lung tissue increases the thoracic pressure above atmospheric pressure. Travelling along the pressure gradient once again, air is pushed out of the lungs (expiration). All of this is controlled by electrical impulses from the central nervous system [**24**].

## 2.4   Control System

The respiratory muscles, like typical skeletal muscles require electrical stimulation from the central nervous system (CNS) to contract [**25**]. The two main muscles of inspiration, the diaphragm and the external intercostal muscles are innervated by the phrenic nerve and the thoracic nerves respectively. Efferent signals travel through these nerves from centers in the brainstem [**26**].

### 2.4.1  Respiration Centers in the Brain

The basic, involuntary rhythm of respiration is produced in centers within the medulla oblongata [**27**]. These are located in the reticular formation of the medulla and are two dense bilateral aggregations of neurons known as the dorsal respiratory group (DRG) and the ventral respiratory group (VRG) (Figure 5).The neurons for inspiration and expiration are both present in each of these aggregates of neurons.

The DRG mainly consists of inspiratory neurons. It is believed that these neurons initiate the contraction of the diaphragm. The VRG sends signals to the muscles of the larynx, pharynx and tongue and maintains an open upper airway. During forced expiration, the expiratory cluster of neurons in the VRG and DRG innervates the internal intercostal muscles, the abdominal muscles and other accessory muscles, along with sending inhibitory signals to the inspiratory muscles. However, during regular (passive) respiration, the expiratory neurons in the VRG only send inhibitory signals to the DRG neurons stopping the excitation of the inspiratory muscles. As a result of the inhibition, the diaphragm and external intercostal muscles relax and the thoracic pressure beings to increase as the lungs recoil and passively expel air out of the respiratory system [**6**].  Both the DRG and VRG receive signals from higher brain centers and various sensory nerves for them to send action potentials (electrical signals) to inspiratory/expiratory muscles.
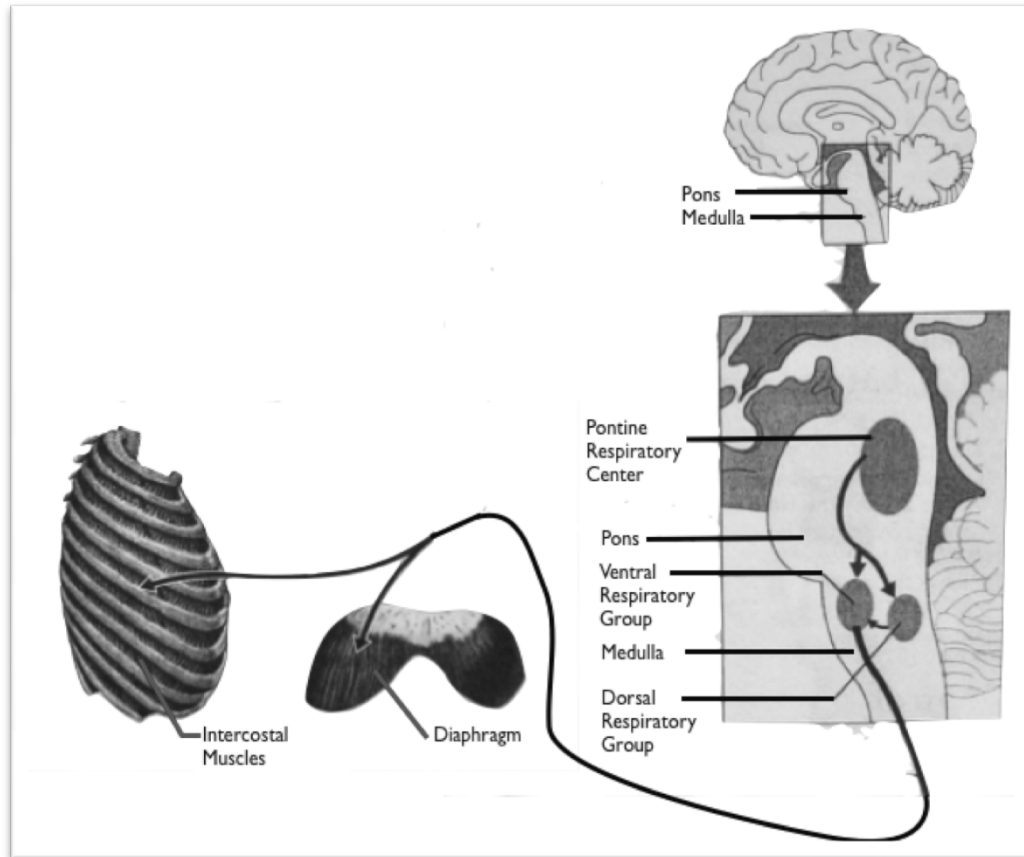
**Figure 5. Respiratory control center – brainstem [6]**

Another important control unit lies in the center known as the pons and is called

the pneumotaxic center [**12**]. This center is believed to fine-tune the breathing rhythm by

influencing the VRG and ensuring a smooth transition between inspiration and

expiration. The rhythm is controlled based on peripheral sensory signals and voluntary

control from higher brain centers. The sensory signals determine the drive of the body for

more oxygen and for removal of carbon dioxide [**25**]. The higher brain center controls

determine the action to be taken during complex activity such as speaking, eating, singing

or exercising.

### 2.4.2  Depth and Rate of Breathing

Adjusting the number of active motor neurons serving the respiratory muscles modifies the depth of respiration; recruiting more motor neurons would provide a larger signal, translating to greater muscle contraction [1]. Regulating how long the inspiratory and expiratory neurons are active can control the rate of breathing. The brainstem adjusts the rate and depth of breathing as a response to the body's demands.

### 2.4.3  Fluid-Chemical Influences on Breathing

The brainstem respiratory centers are sensitive to levels of $CO_2$, $O_2$ and $H^+$ within body fluids [14]. Sensory nerves known as "chemoreceptors" send afferent signals to the medulla and pons about the status of arterial blood and cerebrospinal fluid. Central chemoreceptors are bilaterally located in the ventrolateral medulla (reporting cerebrospinal fluid status) while peripheral chemoreceptors lie in the aortic arch and carotid arteries (reporting $CO_2$, $O_2$ and $H^+$ levels in the blood). Though the levels of these three chemicals are interrelated, the level of $CO_2$ is most closely controlled within the respiratory system [24]. Arterial $CO_2$ passes into the cerebrospinal fluid and hydrates to form carbonic acid. This immediately lowers the pH of the fluid, forcing the depth and rate of breathing to increase. This increased ventilation would become normal when arterial $CO_2$ levels are restored, normalizing cerebrospinal pH.

In some cases, $CO_2$ levels are no longer the primary stimulus. Some pulmonary diseases cause a chronically increased level of $CO_2$ in blood. When this happens, the body adjusts to the new levels and respiration rate is not as sensitive to $CO_2$ anymore. Instead, arterial $O_2$ levels become the primary stimulus. Similarly, without affecting arterial $CO_2$ levels, certain metabolic processes lower blood pH. The respiratory control

system would increase the rate and depth of breathing to compensate for this drop in pH until equilibrium is reached.

### 2.4.4 Higher Brain Center Influences on Breathing

Respiratory rate and depth can also be affected by strong emotions such as excitement, anger, fear and pain [28]. These controls come from a region of the brain superior to the brainstem, known as the hypothalamus. These are involuntary controls that come from the hypothalamus based on the state of mind of the person as well as body temperature.

Along with the involuntary controls to the respiratory system, we can consciously control the rate and depth of breathing [25, 26]. These controls come from the cerebral motor cortex and completely bypass and override (inhibit) the medullar control of the respiratory muscles. The conscious control can be maintained until concentrations of $CO_2$ within the body become critical. When this happens, the medulla takes over and forces higher breathing rate and depth to normalize $CO_2$ levels once again.

### 2.4.5 Other Receptor Influences

Similar to the chemoreceptors, the respiratory system has a variety of other receptors that send afferent signals to the brainstem. One such group is known as stretch receptors [16]. These are located within the pleurae as well as the conducting airways in the lungs. When the lungs are inflated, these receptors send afferent signals through the vagus nerve to the medulla initiating inhibitory signals that end inspiration and prevent the lungs from over-stretching and tearing.

Another larger group of sensors are known as irritant receptors. These are located generously throughout the entire respiratory system. Their main purpose is to detect and

force expulsion of foreign objects such as dust, debris, smoke and other fumes by triggering a sneeze or cough reflex. Regardless of the irritant type, the reflex pattern is always the same. On detecting the irritant, the receptors send afferent signals to the medulla via the vagus nerve. The medullar centers then initiate a deep inspiration, followed by the closing of the glottis before expiratory muscles are innervated. As the abdominal and intercostal muscles contract, the thoracic pressure is greatly increased followed by the sudden opening of the glottis forcing out air from the lungs. If the irritant was detected inferior to the pharynx, the air will be forced out of the oral cavity (cough). If however, the detection were in the nasal cavity, then the tongue and soft palate would close off the oral cavity, forcing air out the nasal passage (sneeze).

One final involuntary reflex is called singultus, commonly known as hiccups. It is believed that this is a remnant of a primal reflex. The afferent and efferent respiratory nerves have a central connection through the cervical spinous processes between the 3rd and 5th cervical vertebrae. Due to a variety of different causes, these nerves form a reflex arc that repetitively contracts the diaphragm and intercostal muscles, along with glottis closure. Normally, this continues until the irritation is no longer present, however, some extreme cases do exist where patients have chronic hiccups. In such cases medical intervention is crucial [26].

## 2.5  Measuring Respiratory Health

The standard stethoscope has limitations in terms of subjectivity of the device as well as which frequency bands are made audible by a specific stethoscope design [29]. Thus alternative, more objective methods of determining respiratory health have evolved. Numerous methods are utilized to measure lung function (pulmonary function testing –

PFT). The various devices used will be explained in detail in the next section, while here we discuss the main non-invasive tests; spirometry and body plethsymography [30]. The main purpose of measuring lung function is to identify and diagnose respiratory diseases and disorders such as asthma, airway hyper-responsiveness, chronic obstructive pulmonary disorder, etc.

The most commonly used spirometry test involves a maximum-effort forced expiration [31]. In order to complete the test properly, the patient must be sitting upright and breathing through a spirometer (Figure 6). After a full inspiration (full lung inflation), the patient must forcefully expire and continue to expire for approximately 6 seconds until all of his/her expiratory reserve volume is expelled.

The spirometer then produces a flow vs volume curve/loop, from which the following variables are measured:

- $FEV_1$  – Forced Expiratory Volume in 1 second [L]
- FVC  – Forced Vital Capacity [L]
- PEF  – Peak Expiratory Flow [L/s]
- $FEF_{50}$  – Forced Expiratory Flow at 50% of FVC [L/s]

These values are then compared to standards set for healthy subjects for the same gender, height, weight, age and ethnic background of the patient [32] to determine the health status of the patient. Another test, body plethysmography, provides additional information on top of those from spirometry; total airway resistance and absolute lung volume [33]. As can be seen from the figure, body plethysmography involves performing controlled breathing maneuvers within an airtight, enclosed chamber.
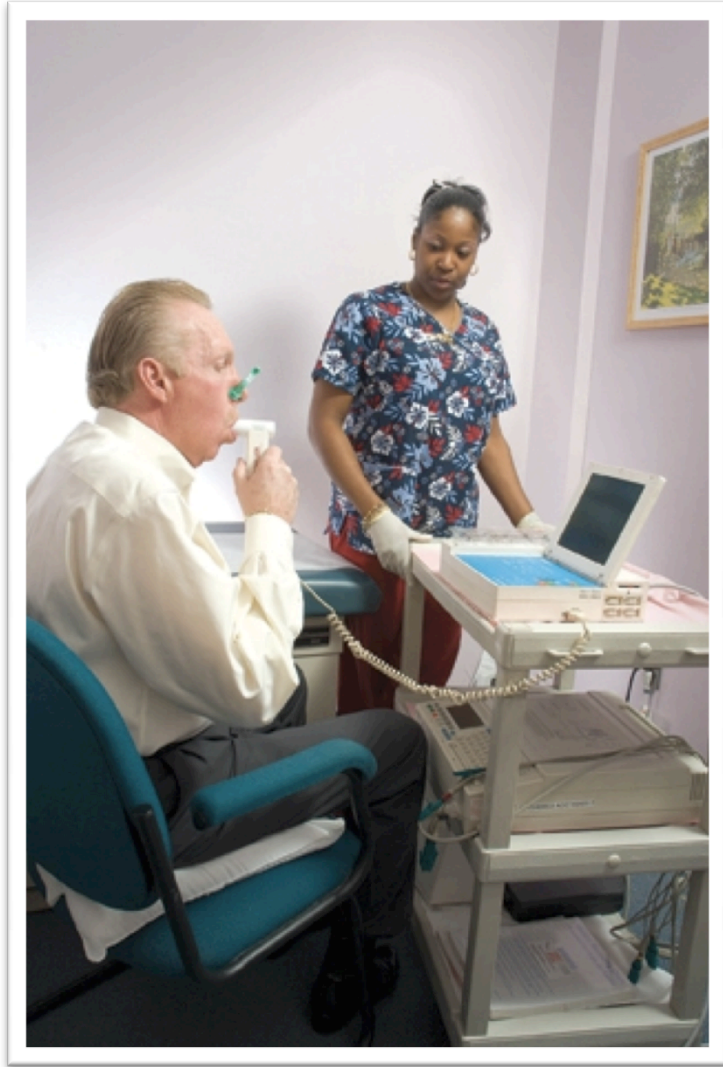
**Figure 6. Spirometry [34]**

Polysomnography (Figure 7) is yet another standardized test used to detect respiratory disorders during sleep. During polysomnography, a patient spends at least one night at a sleep clinic where various physiological signals are recorded from the patient during the entire sleeping period [30]. These signals include ECG, EEG, EMG, thoracic and abdominal movement, $SaO_2$, and sound signals including ambient and snore sounds.
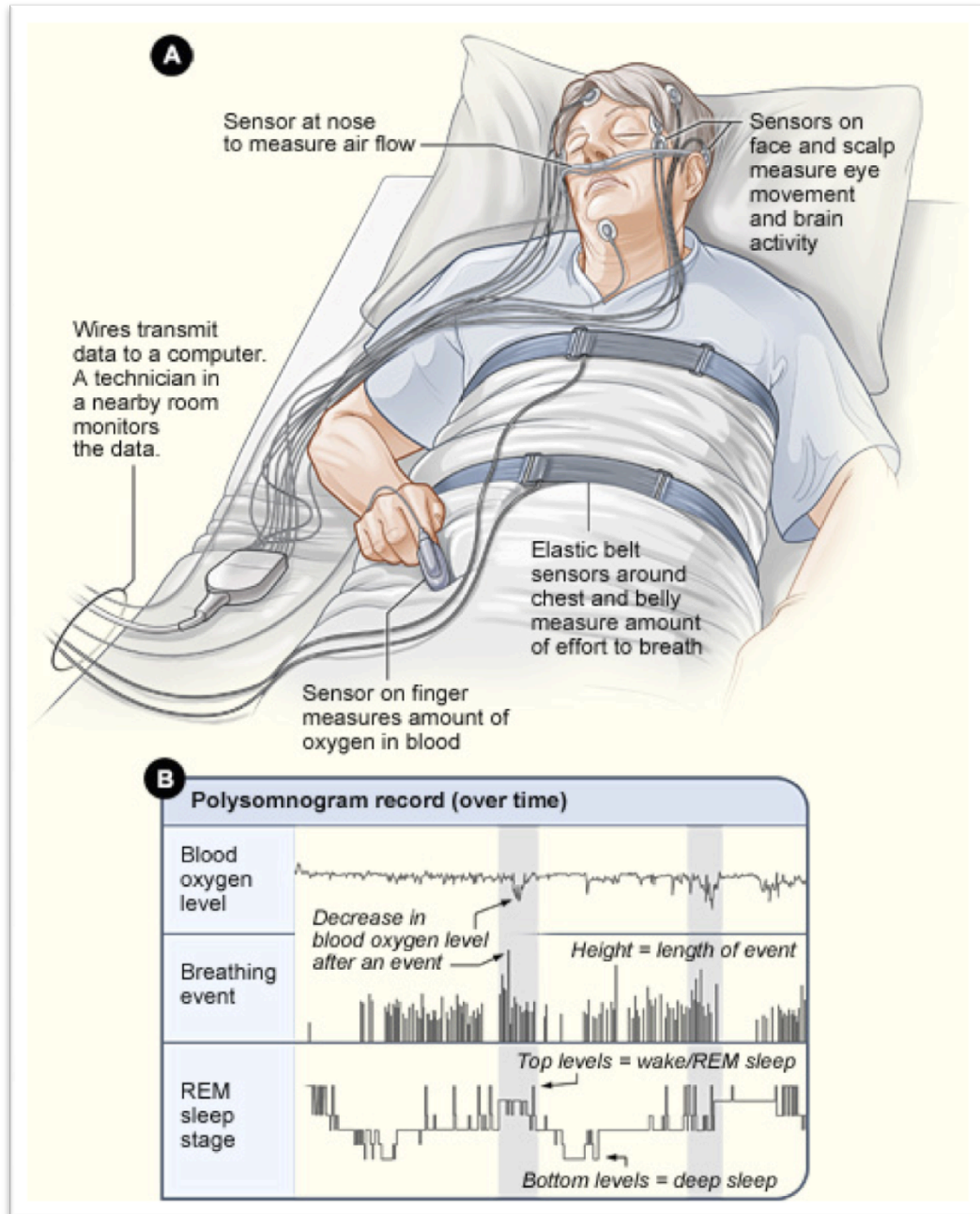
**Figure 7. Polysomnography [35]**

Body plethysmography and polysomnography are comparatively expensive tests. Both require a lot of space for the large equipment and obvious higher cost factors that tie in with the equipment, maintenance and necessary training of a technician for data-processing. Spirometry, by comparison is a more economical test, which explains why it

21

is more popular [**31**]. Nevertheless, all three tests require significant cooperation and understanding from the patient.

## 2.6  Methods used to Monitor Respiration

Respiratory flow can be measured by a variety of different direct and indirect methods. Depending on the situation and available hardware, the extent of use of these flow measurement devices varies. Direct flow measurement devices are those that measure air flowing through the sensor. Indirect devices measure body movements due to respiratory muscles. The following lists the commonly known standard flow measuring devices.

### 2.6.1  Nasal Cannulae

A nasal cannulae is often used in clinical settings to deliver oxygen or supplemental air to critical patients who have trouble breathing. The cannulae itself is a plastic tube that loops around the ears and has two prongs that open into the patient's nostrils as shown in Figure 8. It may also have a supplemental tube for the mouth. A typical nasal cannulae is often connected to oxygen tanks or a hospital's wall outlet for mixed air when used as a breathing aid. For flow measurement purposes, the cannulae is often connected to a flow sensor instead of air supply. The nasal prongs capture minute fluctuations of air, which the flow sensor then determines as respiration.
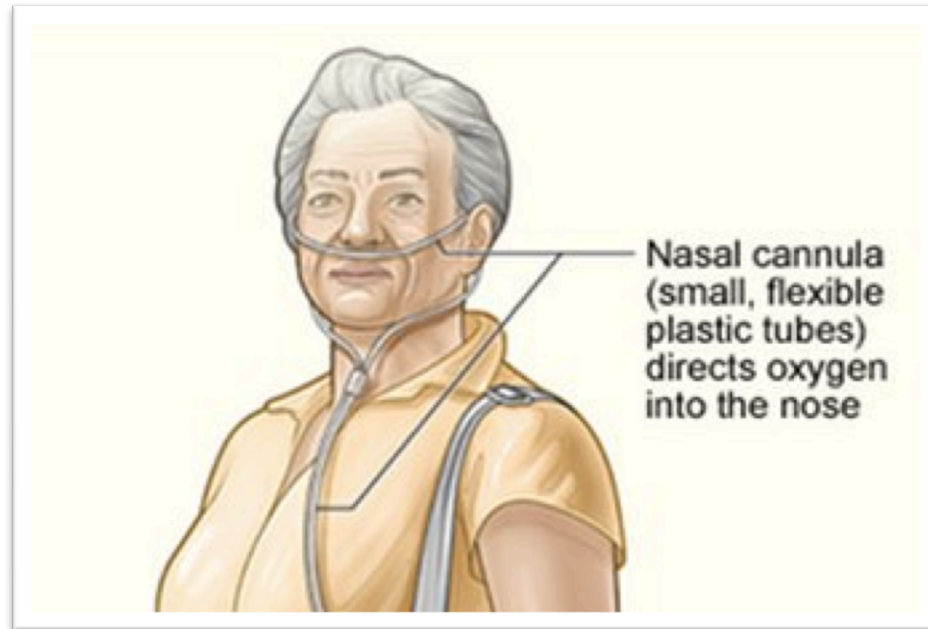
**Figure 8. Nasal cannulae [36]**

There are some limitations to the airflow measured by nasal cannulae [**37**]. Firstly, if the patient breathes orally, then a nasal cannulae will be unable to register the breaths. Another issue is that the nasal prongs are never an airtight fit in the nostrils. As such much of the breathed air escapes from around the prongs during breathing. So a cannulae can at most be used for directional/qualitative information about breathing (whether inspiration or expiration phase) when no oral breathing is involved, but not quantitative or volume analysis of the gas exchange.

### 2.6.2 Spirometer

A spirometer (pneumotachometer) is often used in clinical settings to do pulmonary function tests (Figure 6). This apparatus has a pressure sensor connected to the mouth-piece filter that measures the air flow through the tube. The flow rates and volume estimates gathered from a pneumotachometer are very precise. The limitation of this device however is that the patient has to be conscious during the experiment and has

23

to make sure no breathed air leaks out from around the mouth-piece or from the nostrils [**37**]. This becomes particularly difficult with infants, neurologically-impaired patients or for any long-term (e.g. sleep study) recording where keeping constant, tightly sealed lips around a mouth-piece becomes tedious or impossible.

### 2.6.3  Resistance Bands

These are elastic bands that are designed to go around the torso of a patient. They detect movement by varying their electrical resistance as their length changes. Figure 9 shows a typical resistance band setup. These are placed over the chest and/or abdomen of the patient [**38**]. As he/she breathes, the movement of both the rib-cage and the abdomen are detected as 'respiratory effort' by the bands. This is particularly misleading at times when the patient coughs or there is abdominal movement with no air exchange. Researchers have used different techniques on resistance-band signals, but none that gave reliable breath-flow estimation [**37**]. The inaccuracies of these devices do not allow for volume estimations, let alone determining the proper phase of breath.
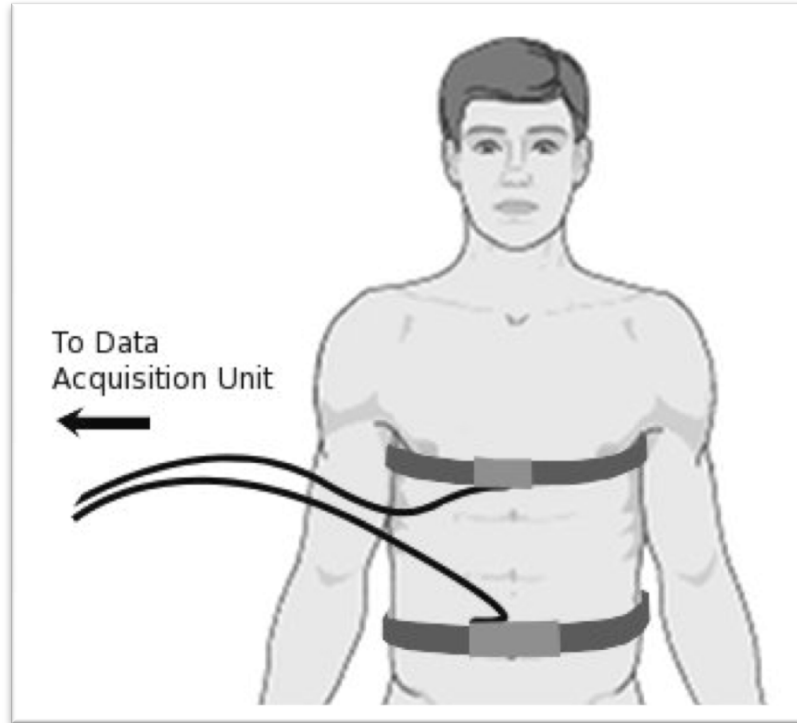
**Figure 9. Resistance band schematic showing chest & abdominal bands**

Presently, in studies that require continuous respiratory flow monitoring, such as sleep studies, nasal cannulaes or resistance bands (or sometimes a combination of both) or facemask spirometer are used. However, nasal cannuale and resistance bands have major disadvantages such as inaccuracy and lack of reference point [4, 5, 39]. Also, breathing through a facemask is inconvenient and adds to the airway resistance. As a result, acoustical flow estimation has gained more interest as an alternative respiratory flow monitoring method [8, 9, 40-42].

## 2.7   Respiratory Acoustics

Respiratory sounds are usually recorded over trachea and/or lungs by a small microphone; each recording location highlights different characteristics of the respiratory sound signals [**43**]. For acoustical flow estimation purposes, the tracheal respiratory

sound signal is preferred because of its high intensity and sensitivity to changes in respiratory flow in comparison to lung sounds [**44**]. In addition, acquiring a clean lung sound signal has practical limitations.

A crucial step in acoustical flow estimation is determining the correct breath phase (inspiration/expiration). Determining breath phases from the lung sounds is a relatively easy task as the breath sound intensity during inspiration is significantly higher than that during expiration; hence, it results in 100% accuracy in respiratory phase identification [**9**]. However, this characteristic is not exhibited in tracheal sounds. Several signal processing methods have been applied to tracheal breath sounds, however, so far using lung sounds have been the only way of breath phase identification [45-48]. Hence, the current flow estimation method requires two channel recording: tracheal sounds for flow estimation and lung sounds for breath phase identification.

For continuous respiratory monitoring such as acoustical sleep apnea monitoring [30, 49], it is desired to record only tracheal sounds. Therefore it would be advantageous to identify breath phases from tracheal sounds only. During normal and quiet breathing the phases alternate, making it easy to know the breath phase if the first phase of breathing is known as *a priori* knowledge. However, this alteration assumption does not hold true for long duration recordings due to non-breathing events, such as apnea, swallow, cough, etc. [**10**]; these non-breathing events can modify the phase alternation in an unpredictable fashion.

As mentioned in previous sections, the flow signal attained by a spirometer is often the most accurate [**42**]. Thus, for comparison purposes, we have opted to record both respiratory sounds simultaneously with spirometric flow. An example of a

respiratory flow signal, measured with a spirometer, and its corresponding filtered

tracheal breath sound signal is shown in Figure 10. The x-axis shows time and the y-axis

shows the flow rate in 'volume per unit time' (L/s). Relaxed, normal respiration, also

known as tidal breathing, has a low frequency often around 0.5 Hz [**44**].
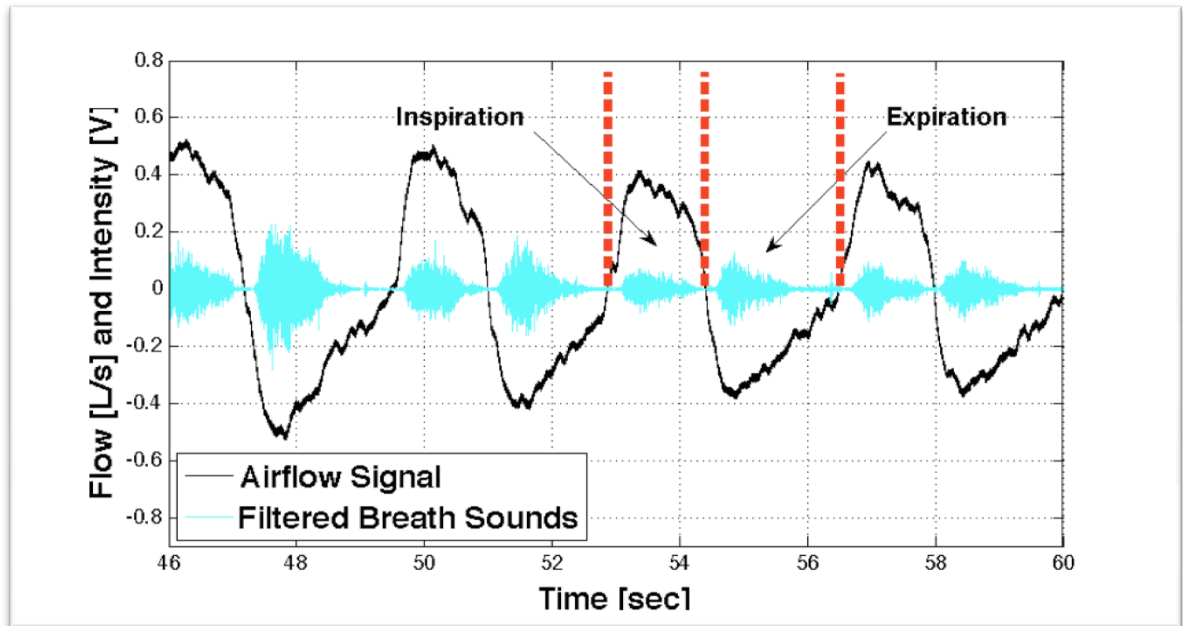


**Figure 10. Typical airflow and filtered tracheal breath signals.**

The main contrast of a flow signal with that of an equivalent acoustic, tracheal

breath sound signal is a difference in the fundamental measuring technique of the

instrument/sensor being used. Respiratory flow measured with a spirometer is a

directional signal. When air flowing through the spirometer changes direction (e.g. breath

phase change from inspiration to expiration) the signal changes sign (e.g. the positive

signal becomes negative). With a microphone however, the acoustic tracheal breathing

signal observed is a result of vibrations. When more air is flowing (i.e. higher flow rate)

the amplitude of the acoustic signal is higher than when less air is flowing through the

trachea. However, the envelope of both inspiration and expiration phases are always positive, as it detects sounds as vibrations – a non-directional unit of measure.

Many flow estimation techniques utilize the envelope of the tracheal sound signal as an approximation for flow rate (refer to Figure 10). With some scaling/calibration, it is easy to see how this can be used for individual phase flow rates.

Several researchers have investigated the relationship between respiratory flow and breathing sounds, and proposed a few flow estimation methods [5, 38, 39, 50-52]. However, all of those methods require both lung and tracheal sounds in order to determine respiratory phases, i.e. inspiration/expiration. Researchers have mused over the possibility of using only tracheal sounds for this analysis. It would require one less input signal, and could simplify acoustic flow determination. We aimed to investigate whether it would be possible to detect respiratory phases using only tracheal breath sounds. Identifying a reliable phase feature that can do this distinction is our goal.

## 2.8 Tracheal Sound Acoustics: Complexity

Breathing rate is controlled by both voluntary and involuntary parts of the CNS. This makes breathing an alternating, yet aperiodic signal. This is also why the duration of individual breath phases shows no significant pattern [38]. The variability in the duration of a breath phase got me to think that this may be a good feature to help distinguish between separate breath phases.

Yet another level of intricacy is the fact that for long-term breathing, the depth of breathing will vary [44]. For our purposes, we have defined 4 distinct flow levels: shallow, tidal, high and very high flow (as discussed in Chapter III). The boundaries have been determined based on the interactions of flow and breath sound within each level.

Under normal circumstances, the expiration phase of a breath cycle is dependent to a large extent on the quantity of air already within the lungs (residual volume – RV). This is indicative of associations between the inspiration and expiration phases of a given breath cycle. This volumetric association and dependence on the RV value, adds to the variability between breath phases [53].

# CHAPTER III

# METHODOLOGY

## 3.1 Approach to Tracheal Breath Analysis

Raw tracheal breath sounds (TBS) experience a lot of interference from various sources of noise[54]. Along with picking up low frequency, ambient noise from the surroundings, the microphone picks up many noises generated from the body, such as gastrointestinal noise and heart sound interference (Figure 11). Most of these disturbances can be removed by simply filtering out audio below a frequency of 150Hz [55]. Heart sounds, unfortunately, have audible elements up to 300Hz, which have strong overlap with tracheal sounds. Thus, filtered TBS will still have effects of noise, specially heart sounds.
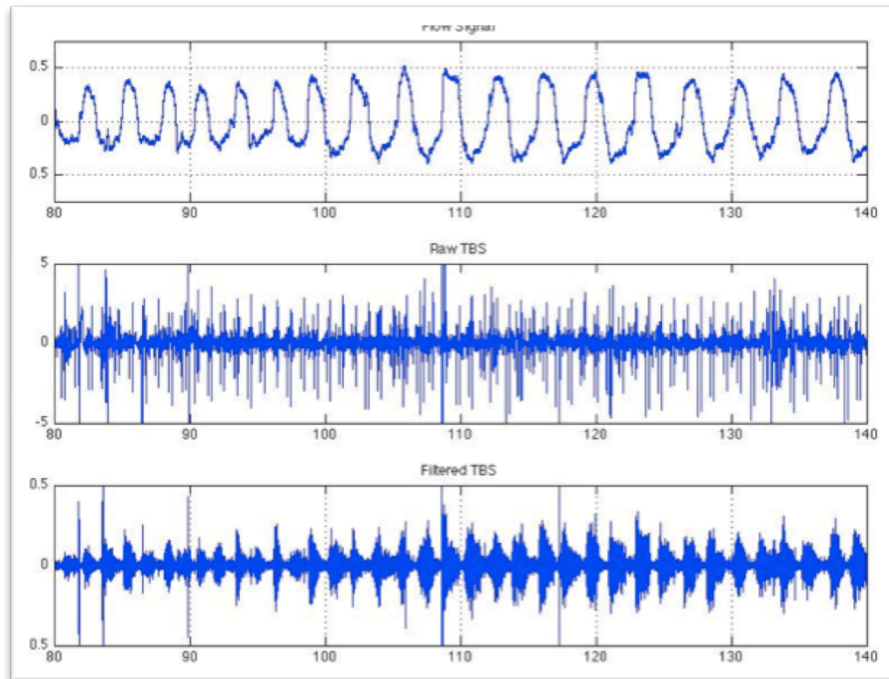


**Figure 11. Flow, raw and filtered tracheal breath sounds**

The most commonly used feature of tracheal breath sound is the average power ($P_{ave}$) of the sound over different frequency bands [56, 57]. It is calculated by estimating the power spectrum of the breath sound signal in 50ms windows with a constant overlap between consecutive windows (50%) over a predefined frequency range[58]. The signal generated by taking the average of the power spectrum within these windows gives $P_{ave}$. Another feature, much similar in concept to $P_{ave}$, is the log-variance of the sound signal [56]. Here, instead of the power spectrum, we calculate the logarithm of the variance of the sound signal within each window, with the same constant overlap between consecutive windows. Both of these features utilize the envelope of the acoustic signal. We've done a comparison study of both these features and found that for our purposes log-variance resulted in better accuracy when looking at different flow levels (shown in Figure 12) [59].
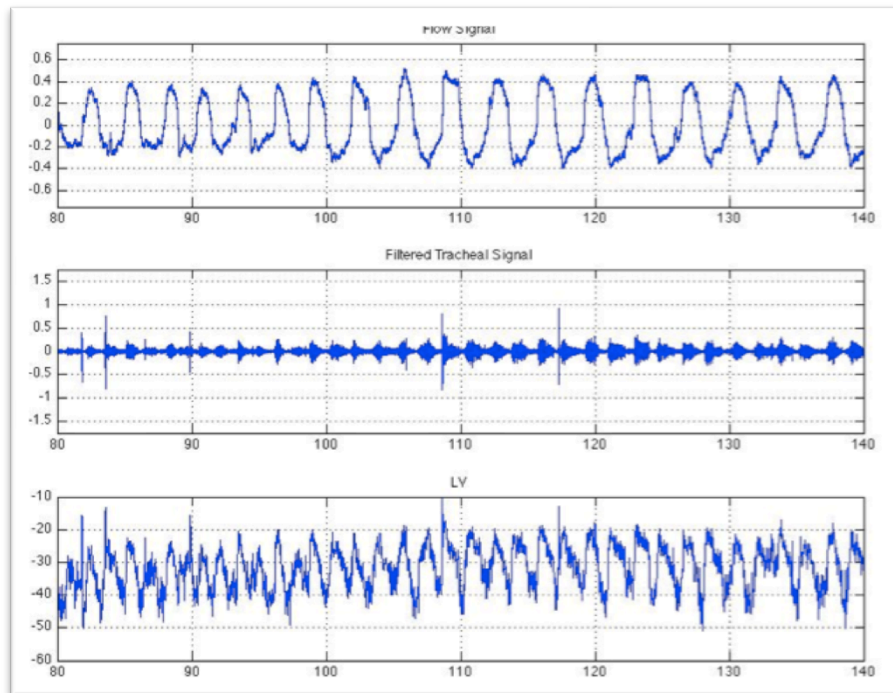


**Figure 12. Flow, filtered tracheal signal and log-variance**

## 3.2    Reasoning for Experimental Setup

Respiration is a cyclical process involving 2 main phases; inspiratory and expiratory. However, the LV or flow-rate signals over a period of time *t* are clearly non-stationary. This is because the quantity of air exchange per unit time varies based on a variety of factors. Primarily the depth of a breath is dependent on the oxygen need of the body. Though we have some control over our own respiration, if the oxygen need is not fulfilled then our involuntary control system takes over and we yawn. The medulla of the brain sends a signal down to the thoracic muscles to increase the thoracic cavity and this forces in more air into the lungs. This semi-control of the respiratory system makes the cyclical process quite varied.
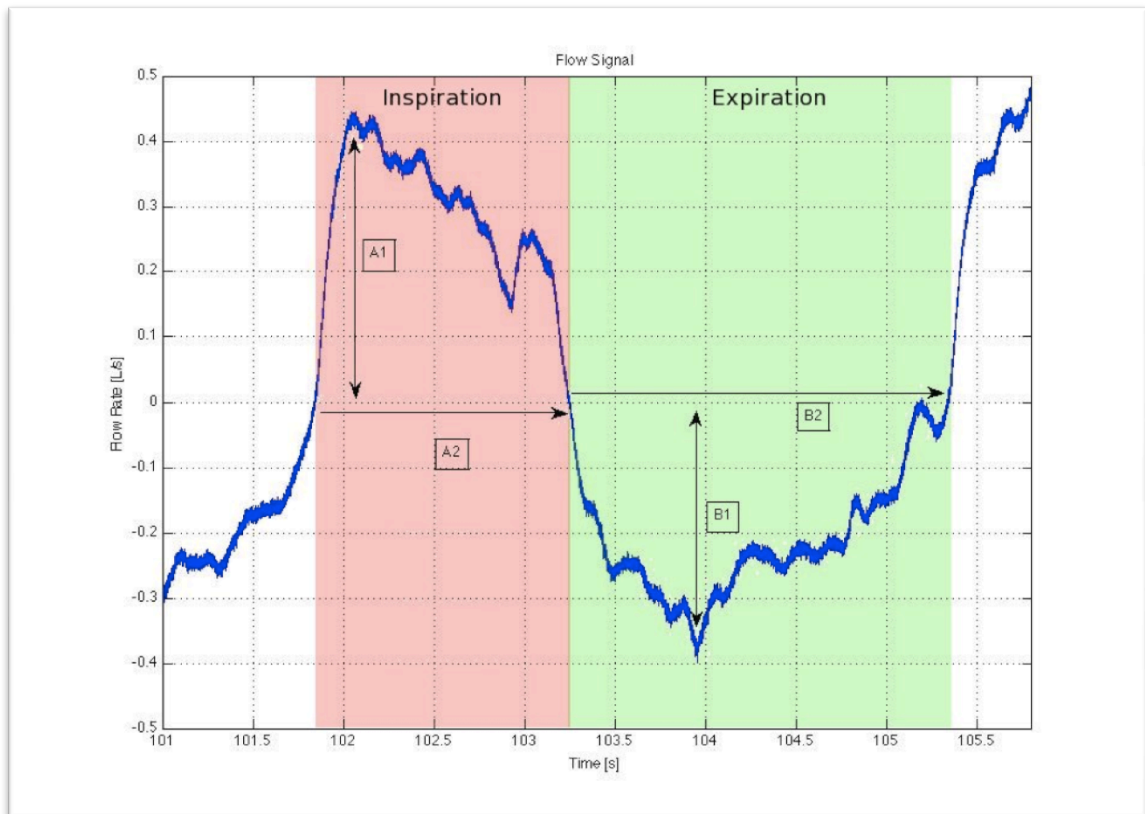


**Figure 13. A typical breath cycle**

Figure 13 above shows a typical single breath cycle, with the inspiration phase in red and expiration cycle in green. Though the quantities themselves may vary, certain key values are of importance. From here we see that 'A1' is the maximum flow-rate of inspiration while 'B1' is the maximum flow-rate of expiration measured in litres per second. 'A2' and 'B2' are the time durations of the phases measured in seconds. During sustained breathing it is often seen that A2<=B2. It is believed that this relationship is most often true since inspiration is an active process, using energy, while expiration is a passive process, using the natural tensile-strength of lung tissue to recoil. Another crucial aspect of sustained breathing is that the volume of air entering the body during inspiration is assumed to be the same as the volume of air leaving the body during expiration. This ensures that the residual volume of air within the lungs is constant. In order to do this, often A1>=B1. Though these relationships are true for majority of breath cycles during long-term sustained breathing, they vary unpredictably for individual breath cycles.

Human beings breathe in a variety of different breath flow levels (Figure 14). Our normal breathing, often the easiest sustained breathing pattern, is known as tidal flow or flow level 2 [FL2: 7.5-15 mL/(s.kg)]. During minimal exertion we breathe slightly deeper, at level 3 [FL3: 15-22 mL/(s.kg)]. After a quick sprint we often breath at the highest breathing level, flow level 4 [FL4:>22 mL/(s.kg)]. This is very high breathing and is often done to compensate for high oxygen demand of the body. This level of breathing cannot be maintained for a long time. During sleep, we often have very little need for oxygen and our breathing naturally falls to a shallow level of breathing [FL1: 0-7.5 mL/(s.kg)]. These are the four flow levels we chose to investigate and study in our attempt to identify phase-distinguishing features from tracheal sounds.
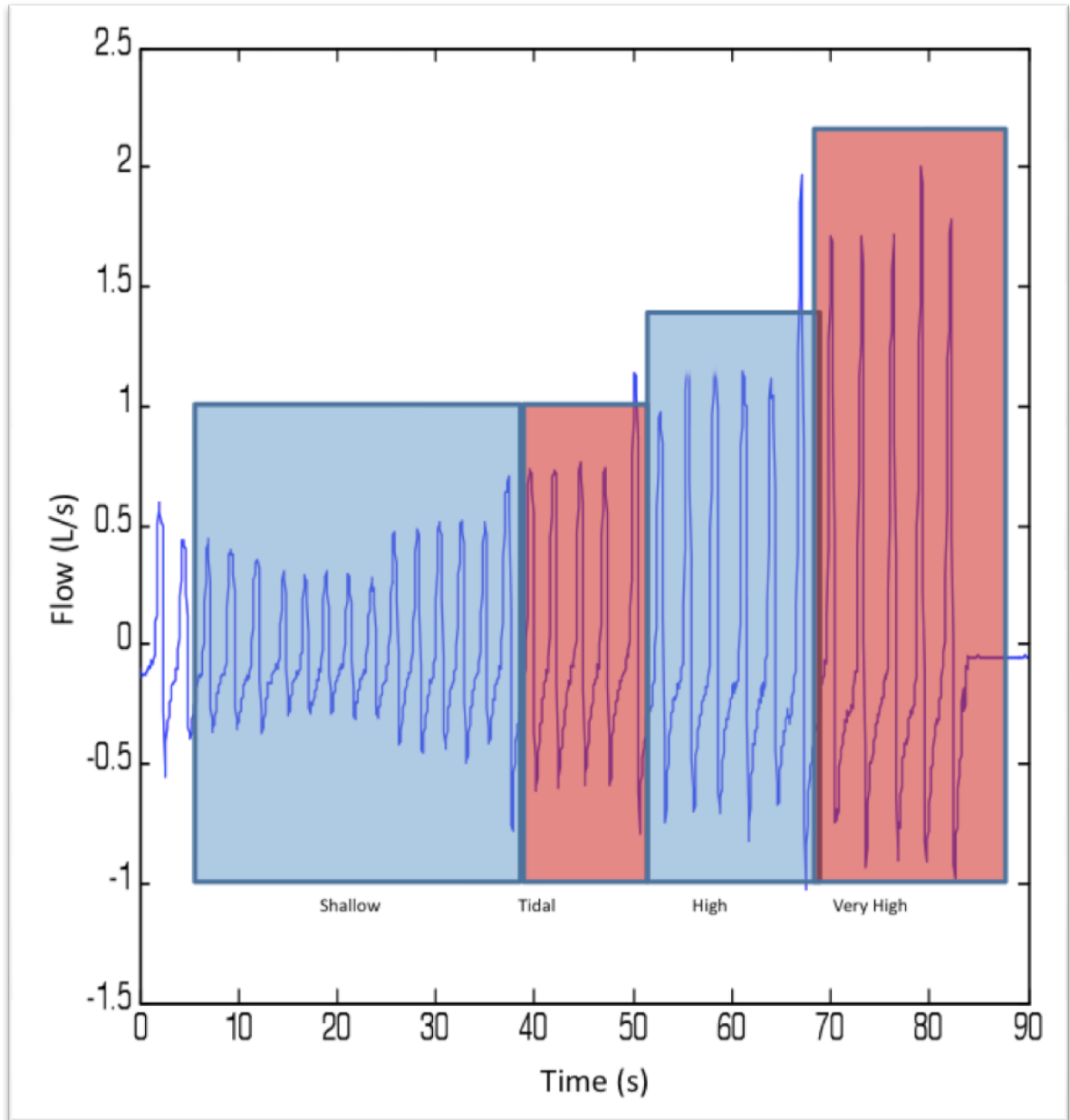
**Figure 14. Typical flow signal at different flow-levels**

## 3.3    Study Participants

Data were collected from 93 healthy participants from a wide age range (41 females, age: 36±12.9 years). The participants were given a questionnaire to fill out before starting the experiment. Since we wanted to create a dataset of healthy subjects, it

34

was important to determine the health of the individuals before they began the experiment [**60**]. Participants were excluded if they answered "Yes" to having a cold, cough or flu or if they were taking medication within 2 weeks prior to the experiment. Participants were also excluded if they had any chronic pulmonary disease such as asthma or chronic bronchitis and had to take bronchodiolators.

They were asked to do a pulmonary function test to determine their baseline FVC and FEV1. From their age, height and gender, their percent-predicted forced expiratory volume in one second (%FEV1) was calculated using the equations below [**61**]:

$$predicted\_FEV1:$$
$$Males \rightarrow 0.04525 \times H - 0.03509 \times A - 2.59946$$
$$Females \rightarrow 0.04071 \times H - 002147 \times A - 2.56958$$

where H: Height (cm)          **Equation 1**
A: Age (years)

$$Percent\_predicted\_FEV1 = \frac{actual\_FEV1}{predicted\_FEV1} \times 100$$

A %FEV1 of below 70% is indicative of a respiratory disorder [**11**]. Only Subjects with a %FEV1 higher than 70% were considered for the experiment. This screening process was important to maintain the strict criteria that the dataset only include breath sounds from healthy subjects.

For later statistical analysis, it was important to determine the activity level of the individual. The participant was asked how many days per week did they exercise on average in the last year. They were given a score from 0-7 inclusive, representing the

number of days per week. They were also asked if they were smokers, and if so, then for how long have they been smoking.

The remaining were physical measurements made on the individuals. Their height was measured in meters, taking the average of 3 trials. Their weight (kg) was recorded using a digital scale. As a standard index value, their body-mass-index (BMI) was calculated by dividing the weight by the square of the height.

The majority of the population following a regular exercise routine; Table II (Chapter IV) shows the demographic information of the participants. None of the participants had any history of major respiratory diseases or disorders. The approval of Biomedical Research Ethics Board of the University of Manitoba was obtained prior to data collection. Also, Prior to recording each participant gave written consent, and completed the simple health questionnaire explained above.

## 3.4   Experimental Procedure

Data recording took place in the acoustic chamber at the Biomedical Engineering Lab, University of Manitoba. The recordings consisted of tracheal breath sounds and respiratory flow signal being recorded simultaneously. These were done during wakefulness, with each recording being approximately 2-5 minutes long.
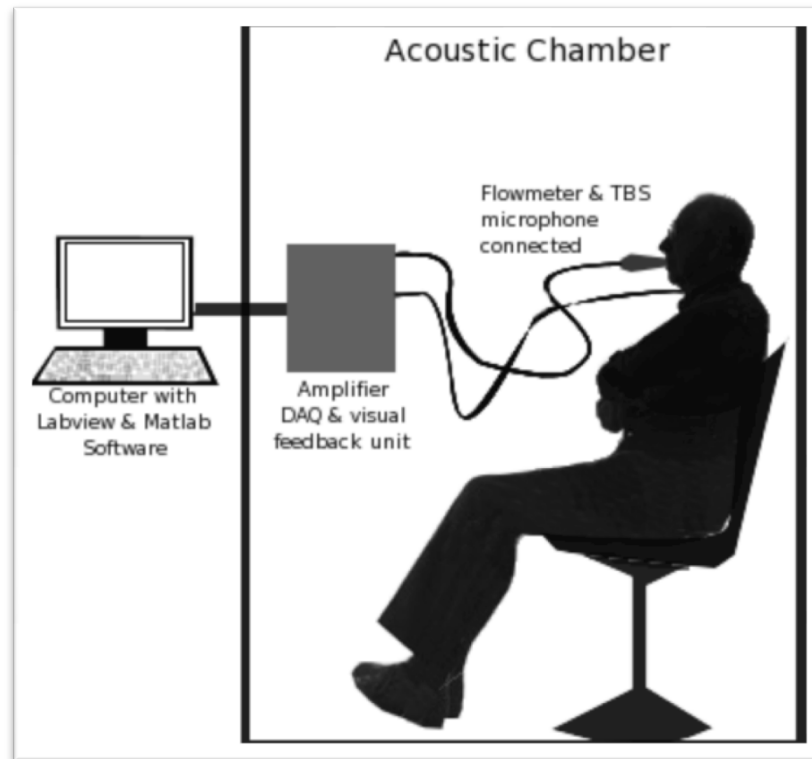
**Figure 15. Schematic diagram of the experimental setup**

Each participant was seated in an upright position, with the flow-meter adjusted to

a comfortable height in front of them, as shown in Figure 15. A standard nose clip was

used to prevent any air escape from the nasal cavity and was kept on throughout the

duration of the experimental recording. The participant was instructed to wrap his/her lips

around the flow-meter mouthpiece, placing the tongue beneath the mouthpiece to provide

the least flow-resistance while breathing orally. The respiratory flow signal of the

participants was shown to them on a monitor to provide visual feedback of their breathing

level. Finally, the microphone was placed in a housing and attached to the base of the

participant's neck (suprasternal notch) using double-sided tape as shown in Figure 16.
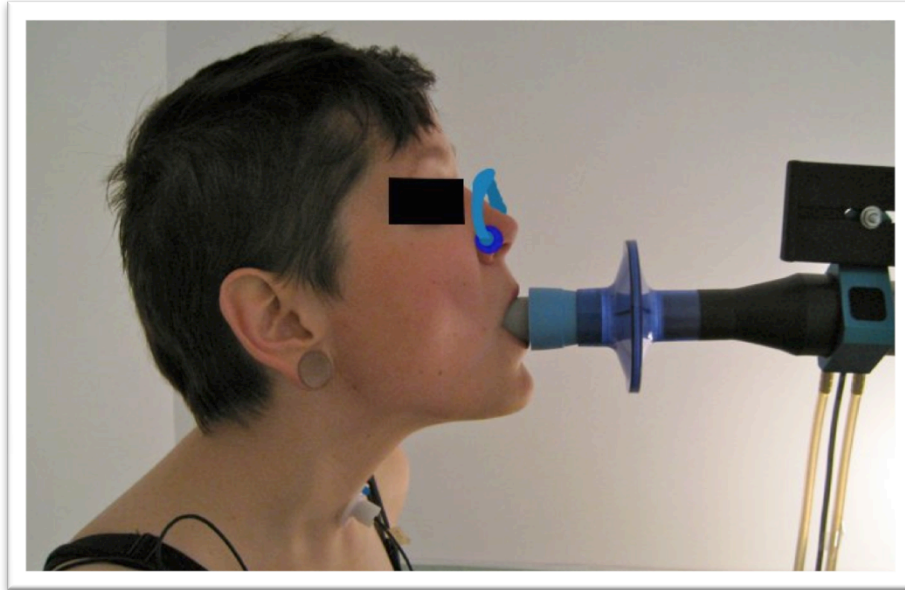
**Figure 16. A participant during the experiment**

Once the participant was comfortable with the sensors and feedback unit, he/she was given visual cues to breathe at four different flow-levels with at least 5 complete breaths at each level. In this study, the flow level were defined as:

- FL1: 0-7.5 mL/(s.kg),

- FL2: 7.5-15 mL/(s.kg),

- FL3: 15-22 mL/(s.kg), and

- FL4: >22 mL/(s.kg).

## 3.5    System Components

Breath sounds were recorded using a Sony condenser microphone (ECM-77B) embedded in a housing with a flat contact surface, 35mm in diameter with a 4mm opening at the center.  The microphone's housing allows a 2 mm air gap between the microphone and the contact surface of the chamber; this ensures that the microphone never touches the skin of the participant during recording. The microphone embedded in

the housing was placed over the participant's suprasternal notch on the neck. The housing was attached to the participant's skin using a double-sided ring tape.

Respiratory flow was measured by a Biopac transducer/flow-meter (TSD127). The breath sound signal was band-pass filtered between 0.05-5000Hz and digitized simultaneously with the flow signal at a 10240 Hz sampling rate. It is important to note that the flow signal was only used as the reference to determine flow level and validate the acoustical breath phase identification.

## 3.6    Signal Processing

### 3.6.1  Preprocessing

The recorded breath sound signal was first band-pass filtered between 150-800Hz, using a $5^{th}$ order Butterworth filter to minimize the effect of heart sounds and high frequency noises (if any) [62]. Figure 17 shows a typical filtered tracheal breath sound signal along with its corresponding flow signal. The onsets of the two breath phases of one full breath cycle (inspiration and expiration) are marked with 3 vertical dashed-lines.

### 3.6.2  Onset Determination

As the first stage, we need to determine the onset of each breath phase on the tracheal sound record. Similar to our previous study [40], the LV parameter was calculated from the filtered sound signals in windows of 25ms duration (256 samples) with 50% overlap between successive windows, using Hanning windows. Figure 18 shows the spectrogram of the same signal shown in Figure 17, along with its calculated LV signal.
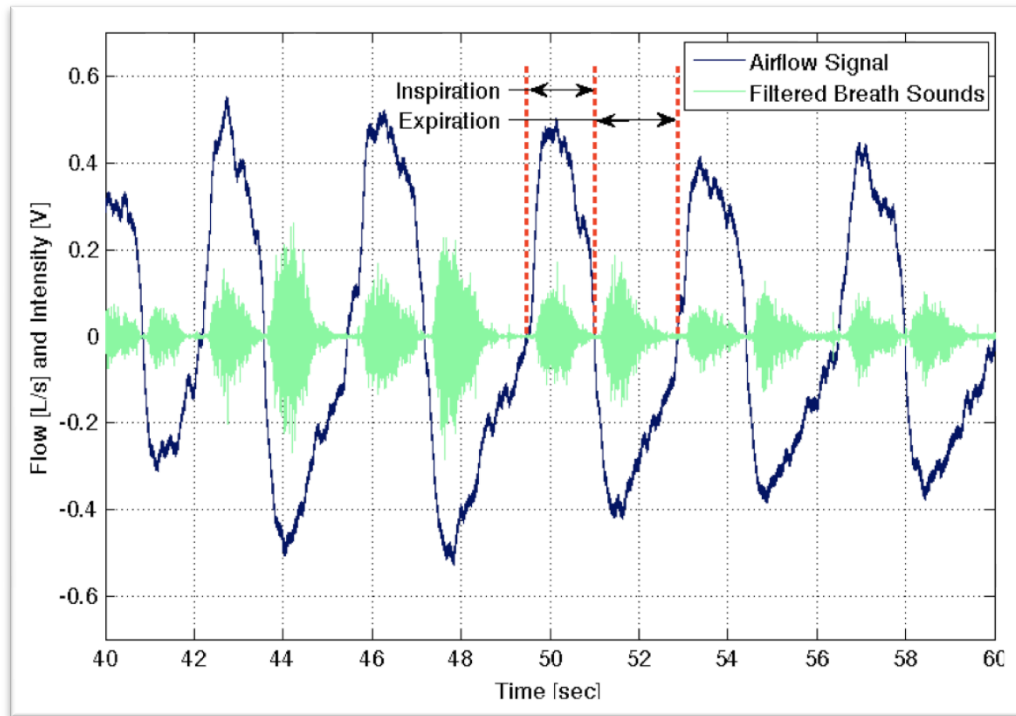
**Figure 17. Flow and filtered tracheal signals. Inspiration and expiration segments of a single breath cycle are indicated.**
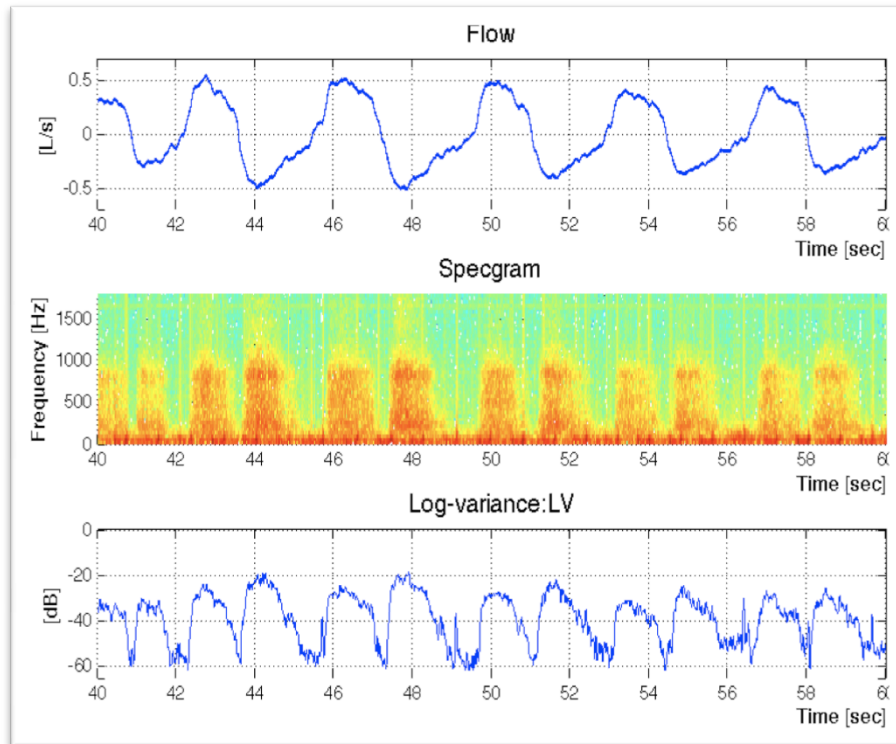
**Figure 18. From top to bottom, medium flow rate samples of the recorded flow signal, the spectrogram of the corresponding raw-tracheal-breath-sounds, estimated LV of the corresponding filtered-TBS in the range [150-800]Hz.**

Note that the LV of the breath sounds resembles a fully rectified flow signal; hence, they can be used to detect breath phase onsets [**40**]. We adopted the same method of onset detection we used in our previous study, where we executed a running window across the LV signal in the time domain. The running window would detect minimas in the signal by observing the instances of change in direction of the signal (sign change). In some cases, where there is some noise near the onset of a phase, there would be a cluster of minimas. In such cases, the algorithm was designed to consider the median value as the 'onset'. This was a highly effective way to detect onsets of breath phases from tracheal sounds (Figure 19). These onsets were then used to separate the entire recording

into a chain of consecutive breath phases. Individual characteristics markers were determined for each phase, which we called Phase-Index (PI) values.
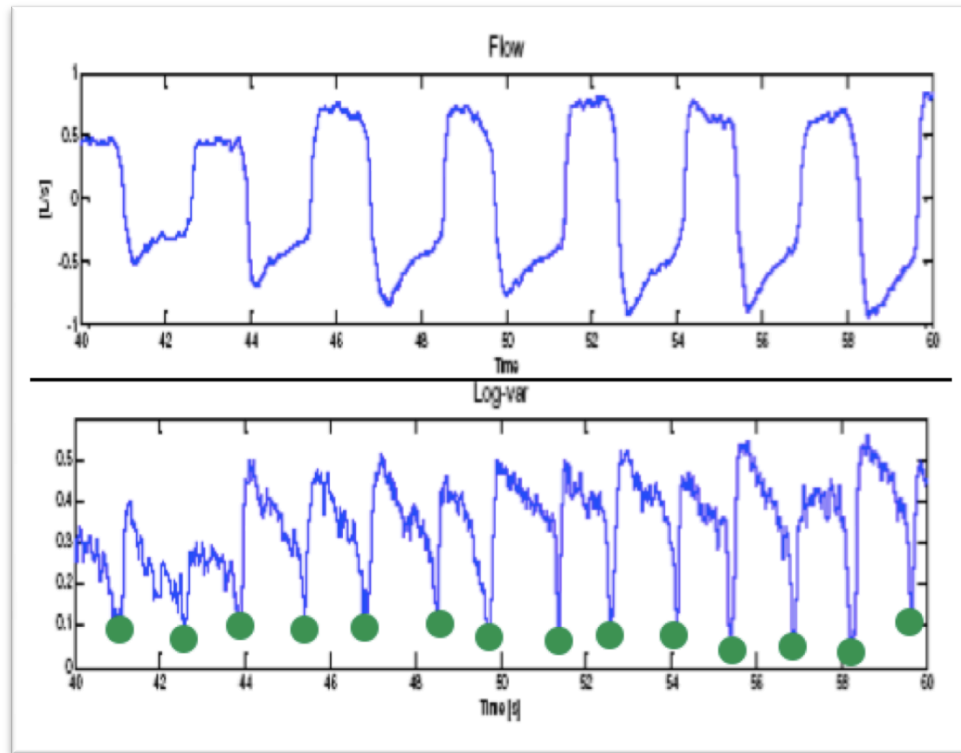


**Figure 19. Onset detection from log-variance**

### 3.6.3 Phase Index Parameters

In this study, we derived five parameters from the breath sounds as the phase index ($PI_x$) parameters; they were calculated for each respiratory phase from its corresponding LV curve (Figure 20).

Once the onsets were determined, a single continuous recording of breathing sound signal was viewed as a chain of separate phases. This segmentation provided a different view to the duration of recordings; it didn't matter if the recording was 5 minutes long or for 5 hours, the phase analysis on each segment would be the same.

42

It was also evident that the envelope of the filtered TBS, the LV signal, contained much of the shape information of the actual breath phase (Figure 20). By visually observing the flow and LV-phase pairs of the first few participants, certain elements of the bell-shape were deemed significant and were termed the Phase-Index parameters.
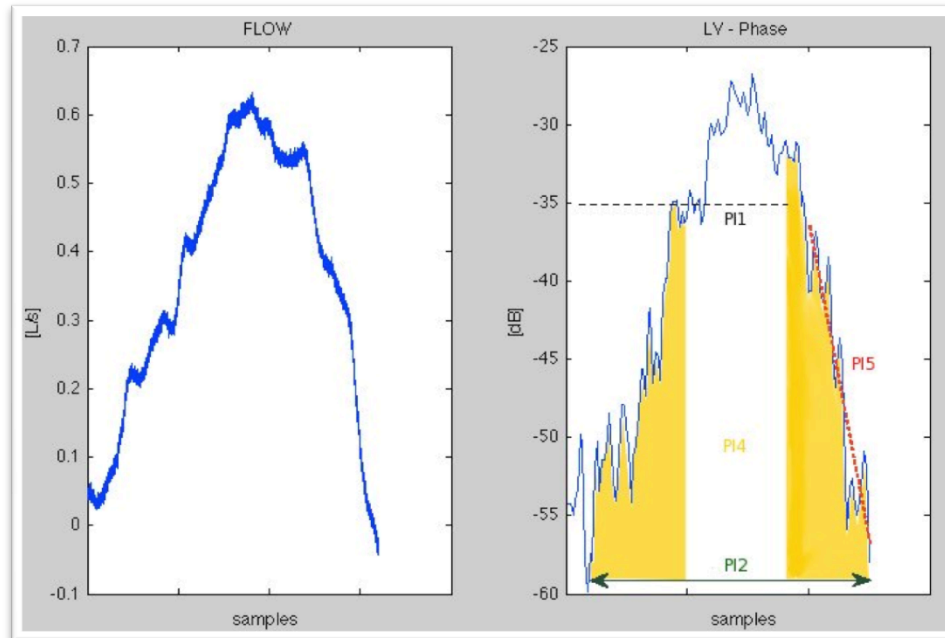


**Figure 20. On the left, a single (inspiratory) phase of the airflow signal at high flow rate. On the right, the corresponding phase's LV of filtered-TBS with indications of the phase indices; $PI_1$, $PI_2$, pseudo-volume index $PI_4$, and falling-gradient index $PI_5$.**

The purpose of deriving the phase parameters is to capture and represent different information about the breath phase. The first phase-index parameter, $PI_1$, is the sound's intensity in each phase. It is calculated by taking the average of the top 20% LV values within the phase. This averaging minimizes the effect of any variance that was not eliminated by the filtration step. This represents the typical approximation of peak intensity (or amplitude) of the breath phase in decibels (dB), and is the most studied parameter of respiratory signals.

$PI_2$ is the duration of the phase measured in seconds. Since the individual breath phases are not normalized, both the intensity and duration parameters hold key information about the general shape of the curve.

The remaining three parameters are our own features that we are introducing in our method. $PI_3$ and $PI_4$ are pseudo-volume parameters, calculated by using the trapezoidal method. $PI_3$ is the percentage of the area under the LV curve in the first half of the phase. For $PI_4$, the phase is sectioned into 3 equal portions in the time-domain and $PI_4$ is the difference between the percentage of the area under the LV curve between the $1/3^{rd}$ and $3/3^{rd}$ sections.

The final phase parameter, $PI_5$, is the falling gradient of the breath phase; it is calculated by fitting a line to the LV values of the last 20% duration of each phase. Figure 20 shows the derivation of these parameters in one breath phase.

### 3.6.4 Voting Method

Once $PI_{1-5}$ values were determined for each phase, the values of these parameters in three consecutive phases (*n-1*, *n* and *n+1*) were considered for the decision making on the current phase (*n*) as shown in equation (1).

$$
\begin{aligned}
V_{1X}(n) &= PI_X(n) - PI_X(n-1); \\
V_{2X}(n) &= PI_X(n) - PI_X(n+1); \\
\rightarrow PI_{X-vote}(n) &= \frac{(V_{1X}(n) + V_{2X}(n))}{(2 * \max(V_{1X}(n), V_{2X}(n))};
\end{aligned}
$$

**Equation 2**

The $PI_{x-vote}$ value determined the label of each phase: if $PI_{x-vote}$ was positive (negative), the phase was labeled as inspiration (expiration). Note that $PI_{x-vote}$ is always a number between 1 and -1, the closer it is to either boundary, the stronger the decision on the phase labeling.

Thus, by going through *'n'* breath phases for every subject, and calculating the individual votes of the five parameters, an *'n x 5'* two-class, decision matrix was generated. The flowchart in Figure 21 shows the steps taken to develop the 'decision matrix'.
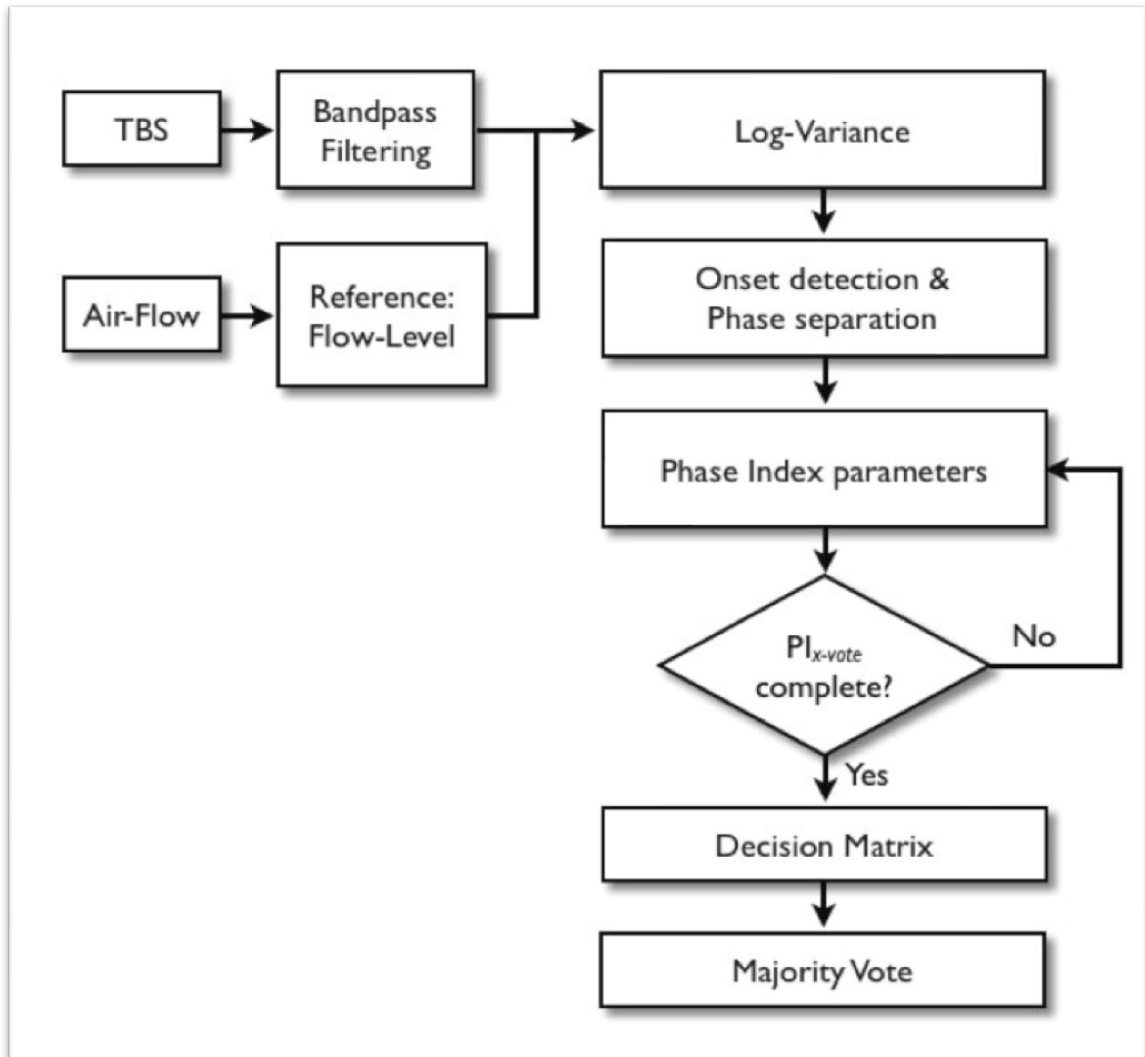


**Figure 21. Flowchart for breath phase detection.**

The performance of this phase detection method was evaluated by calculating sensitivity and specificity of the method, as defined in equation (2). We also investigated the statistical significance of each of the PI parameters by Analysis of Variance

45

(ANOVA) and with Multivariate Analysis of Variance (MANOVA); in call instances $p < 0.05$ was considered significant [63].

$$Specificity = \frac{TN}{TN + FP}$$

$$Sensitivity = \frac{TP}{TP + FN}$$

**Equation 3**

where
TP = Correctly classified inspirations,
TN = Correctly classified expirations,
FP = Incorrectly classified inspirations,
FN = Incorrectly classified expirations

# CHAPTER IV

# RESULTS AND DISCUSSION

The integrity of the dataset was of great importance throughout the development and implementation of this project. As such a large dataset of simultaneous flow-signal and tracheal sound recording at different flow levels from healthy participants did not exist prior to this project. A strict protocol for screening healthy participants was established and followed in development of this dataset as described in detail in section 3.3 and 3.4 of this thesis. The objective of developing this large dataset that adheres to the experimental protocol was achieved.

Table II shows the demographical distribution of the data used for this study. Data are sorted in groups based on the age, smoking and exercise status as well as measured values such as height and weight. Table II also shows the grouping that was used for the multivariate analysis of variance (MANOVA) statistical test. The groups were made based on intuitive boundaries while trying to keep them well balanced/distributed.

**Table II. Demographic information of participants**

**[G$_x$= Group X, mean ± standard deviation: within each group, n=number of participants in group.]**

| ETHNICITY | G$_1$ : Caucasian (n = 48) | G$_2$ : Other (n = 45) | | | | | | |
|---|---|---|---|---|---|---|---|---|
| GENDER [Male, Female] | G$_1$ : Male (n = 52) 55.9% | G$_2$ : Female (n = 41) 44.1% | | | | | | |
| AGE [yrs] | G$_1$ < 25 (n = 19) 22.8 ± 1.9 | 25 ≤ G$_2$ < 30 (n = 20) 27.6 ± 1.3 | 30 ≤ G$_3$ < 35 (n = 17) 32.6 ± 1.8 | 35 ≤ G$_4$ < 40 (n = 11) 37.3 ± 1.2 | 40 ≤ G$_5$ < 50 (n = 16) 45.4 ± 3.0 | G$_6$ > 50 (n = 10) 63.7 ± 10.3 | | |
| HEIGHT [cm] | G$_1$ < 165 (n = 30) 160 ± 10.3 | 165 ≤ G$_2$ < 175 (n = 45) 169 ± 2.5 | G$_3$ > 175 (n = 18) 180 ± 3.1 | | | | | |
| WEIGHT [kg] | G$_1$ < 50 (n = 6) 47.8 ± 2.2 | 50 ≤ G$_2$ < 60 (n = 19) 55.9 ± 2.6 | 60 ≤ G$_3$ < 70 (n = 32) 64.4 ± 2.6 | 70 ≤ G$_4$ < 80 (n = 23) 75.9 ± 2.8 | 80 ≤ G$_5$ 90 (n = 7) 84.7 ± 2.7 | G$_6$ > 90 (n = 6) 95.1 ± 6.0 | | |
| ESTIMATED BMI [kg/m²] | G$_1$ < 18.5 (n = 5) 18.1 ± 0.5 | 18.5 ≤ G$_2$ < 25 (n = 55) 21.8 ± 1.6 | 25 ≤ G$_3$ < 30 (n = 25) 27.1 ± 1.4 | G$_4$ > 30 (n = 8) 32.5 ± 2.7 | | | | |
| EXERCISE [days/week] | G$_1$ :0 (n = 19) | G$_2$ :1 (n = 4) | G$_3$ :2 (n = 11) | G$_4$ :3 (n = 22) | G$_5$ :4 (n = 12) | G$_6$ :5 (n = 13) | G$_7$ :6 (n = 3) | G$_8$ :7 (n = 9) |
| SMOKING [yes, no] | G$_1$ :Yes (n = 15) | G$_2$ : No (n = 78) | | | | | | |

# 4.1   Decision Matrix

Once the $PI_{1-5}$ values were determined, it was important to see which of these values presented enough characteristics to determine the breath phase. In order to do this visually, the decision matrix was created based on the $PI_{x\text{-vote}}$ as shown in equation## in Chapter III. The 'decision' matrix was determined for every subject, with each of the five columns representing one of the $PI_{x\text{-vote}}$, and each row represented one phase. For easy visualization, the decision matrix for each subject was displayed in a color-coordinated table against actual. The votes (matrix elements) were quantized into 4 color-levels, showing 'strength' of the decision with the red and dark blue colors representing 100%

strength in decision on 'inspiration' and 'expiration', respectively. The actual phases were determined from the airflow signal for verification. One such table is shown in Figure 22 along with the color-bar that shows the different levels (strength of the vote). The decision matrix table was generated for every subject.

## 4.2  PI$_x$ Significance Across Different Flow-levels

ANOVA was run to investigate any significant variation of the PI parameters between the four flow levels. For each PI the data was analyzed separately for inspiration and expiration groups, to remove the effect of breath-phase. ANOVA was run on each of the PI between the 4 flow levels and the *p-value* results (significance: $p < 0.05$) of the test are shown in Table III below.

**Table III. ANOVA p-value results – Effect of flow-level on PI parameters**

**[p-value indicates strength of the null hypothesis that "the flow level does NOT affect the PI parameter"]**

|  | PI$_1$ | PI$_2$ | PI$_3$ | PI$_4$ | PI$_5$ |
|---|---|---|---|---|---|
| Inspiration | 0.00 | 0.03 | 0.28 | 0.58 | 0.79 |
| Expiration | 0.00 | 0.00002 | 0.42 | 0.79 | 0.40 |
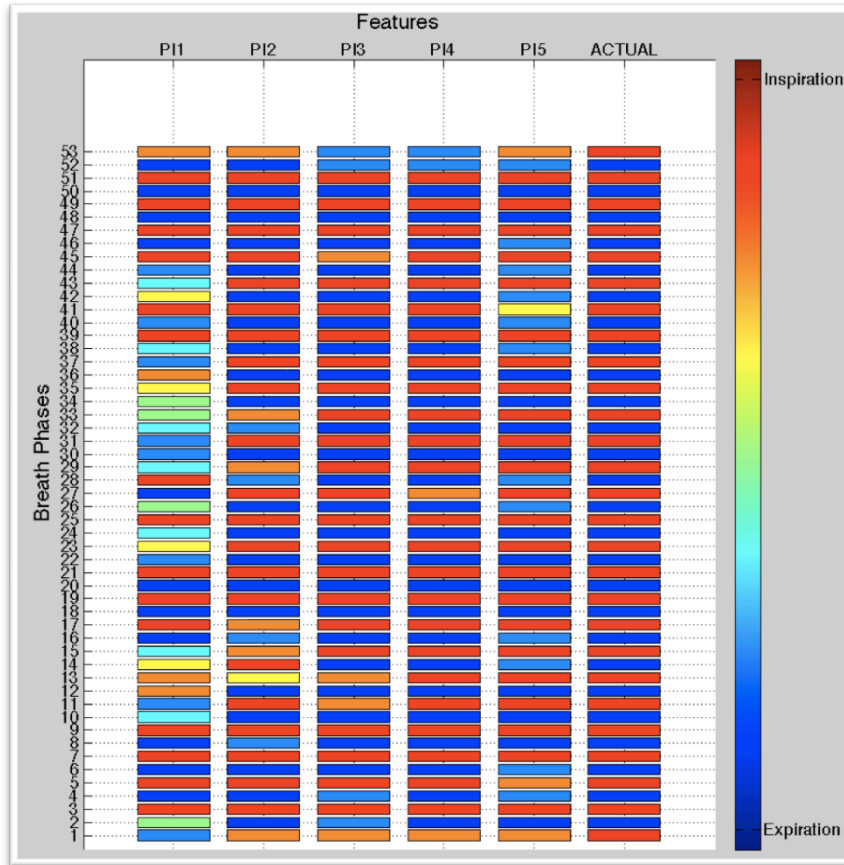
**Figure 22. A typical decision matrix in color-coordinated-table**

## 4.3 Majority/Combined Votes

As a preliminary step, we examined 6 out of the 93 subjects and visually observed the decision matrices. It was clear than no single phase-index was able to stand alone as a phase identification feature. Three parameters showed the highest accuracy in their classification; they were $PI_2$, $PI_4$ and $PI_5$.

Two majority vote approaches, 5VOTE and 3VOTE, were then calculated by taking an equal-weight average of the PI votes. 5VOTE took the majority vote of all five

PIs, while 3VOTE took the average vote of the parameters with the highest accuracy ($PI_2$, $PI_4$ and $PI_5$).

From the preliminary study, it was seen that the 3VOTE method was superior in performance to the 5VOTE majority method [40]. That is why the main focus was on the results from the 3VOTE method. When this was run on the entire dataset of 93 subjects, the 3VOTE phase detection method yielded very high performance (Sensitivity: 95.5%, Specificity: 95.6% and Accuracy 95.6% shown in Figure 23).

Table IV shows detailed results of the 3VOTE phase detection method, with the performance indicators (sensitivity, specificity and accuracy) of the detection for each individual participant. The average performance indicators are also included.

**Table IV. Summary of results for individual participants**

[table continued on next page] - PID=participant identification number, NOP=total number of phases, NAI=total number of actual inspirations, TP=number of true positives, FP=number of false positives, FN=number of false negatives, Sn%=sensitivity, Sp%=specificity, Acc%=accuracy.

| PID | NOP | NAI | TP | FP | FN | 3-variable-vote | | |
| --- | --- | --- | --- | --- | --- | --- | --- | --- |
| | | | | | | Sn % | Sp % | Acc % |
| 1 | 77 | 38 | 38 | 0 | 0 | 100.0% | 100.0% | 100.0% |
| 2 | 81 | 40 | 40 | 0 | 0 | 100.0% | 100.0% | 100.0% |
| 3 | 63 | 31 | 30 | 1 | 1 | 96.8% | 96.9% | 96.8% |
| 4 | 82 | 41 | 39 | 3 | 2 | 95.1% | 92.7% | 93.9% |
| 5 | 78 | 39 | 39 | 0 | 0 | 100.0% | 100.0% | 100.0% |
| 6 | 72 | 36 | 32 | 3 | 4 | 88.9% | 91.7% | 90.3% |
| 7 | 76 | 38 | 38 | 0 | 0 | 100.0% | 100.0% | 100.0% |
| 8 | 54 | 27 | 26 | 0 | 1 | 96.3% | 100.0% | 98.1% |
| 9 | 64 | 32 | 32 | 0 | 0 | 100.0% | 100.0% | 100.0% |
| 10 | 75 | 37 | 37 | 0 | 0 | 100.0% | 100.0% | 100.0% |
| 11 | 44 | 22 | 21 | 0 | 1 | 95.5% | 100.0% | 97.7% |
| 12 | 82 | 41 | 41 | 0 | 0 | 100.0% | 100.0% | 100.0% |
| 13 | 87 | 44 | 43 | 0 | 1 | 97.7% | 100.0% | 98.9% |
| 14 | 76 | 38 | 38 | 0 | 0 | 100.0% | 100.0% | 100.0% |
| 15 | 63 | 31 | 30 | 1 | 1 | 96.8% | 96.9% | 96.8% |
| 16 | 92 | 46 | 46 | 0 | 0 | 100.0% | 100.0% | 100.0% |
| 17 | 60 | 30 | 30 | 0 | 0 | 100.0% | 100.0% | 100.0% |
| 18 | 61 | 30 | 30 | 0 | 0 | 100.0% | 100.0% | 100.0% |
| 19 | 83 | 41 | 41 | 0 | 0 | 100.0% | 100.0% | 100.0% |
| 20 | 72 | 36 | 33 | 2 | 3 | 91.7% | 94.4% | 93.1% |
| 21 | 84 | 42 | 40 | 5 | 2 | 95.2% | 88.1% | 91.7% |
| 22 | 65 | 32 | 31 | 1 | 1 | 96.9% | 97.0% | 96.9% |
| 23 | 75 | 37 | 29 | 9 | 8 | 78.4% | 76.3% | 77.3% |
| 24 | 79 | 39 | 39 | 0 | 0 | 100.0% | 100.0% | 100.0% |
| 25 | 87 | 43 | 42 | 0 | 1 | 97.7% | 100.0% | 98.9% |
| 26 | 82 | 41 | 41 | 0 | 0 | 100.0% | 100.0% | 100.0% |
| 27 | 73 | 37 | 35 | 1 | 2 | 94.6% | 97.2% | 95.9% |
| 28 | 79 | 39 | 37 | 6 | 2 | 94.9% | 85.0% | 89.9% |
| 29 | 68 | 33 | 28 | 7 | 5 | 84.8% | 80.0% | 82.4% |
| 30 | 82 | 41 | 41 | 0 | 0 | 100.0% | 100.0% | 100.0% |
| 31 | 75 | 37 | 37 | 0 | 0 | 100.0% | 100.0% | 100.0% |
| 32 | 87 | 43 | 33 | 10 | 10 | 76.7% | 77.3% | 77.0% |
| 33 | 118 | 59 | 55 | 6 | 4 | 93.2% | 89.8% | 91.5% |
| 34 | 64 | 32 | 32 | 0 | 0 | 100.0% | 100.0% | 100.0% |
| 35 | 77 | 38 | 38 | 0 | 0 | 100.0% | 100.0% | 100.0% |
| 36 | 88 | 44 | 44 | 0 | 0 | 100.0% | 100.0% | 100.0% |
| 37 | 52 | 26 | 25 | 0 | 1 | 96.2% | 100.0% | 98.1% |
| 38 | 72 | 36 | 35 | 0 | 1 | 97.2% | 100.0% | 98.6% |
| 39 | 73 | 36 | 35 | 1 | 1 | 97.2% | 97.3% | 97.3% |

...
...

| PID | NOP | NAI | TP | FP | FN | 3-variable-vote | | |
|---|---|---|---|---|---|---|---|---|
| | | | | | | Sn % | Sp % | Acc % |
| 40 | 74 | 37 | 33 | 5 | 4 | 89.2% | 86.5% | 87.8% |
| 41 | 79 | 39 | 39 | 0 | 0 | 100.0% | 100.0% | 100.0% |
| 42 | 56 | 28 | 28 | 0 | 0 | 100.0% | 100.0% | 100.0% |
| 43 | 82 | 41 | 40 | 1 | 1 | 97.6% | 97.6% | 97.6% |
| 44 | 70 | 35 | 31 | 4 | 4 | 88.6% | 88.6% | 88.6% |
| 45 | 74 | 37 | 37 | 0 | 0 | 100.0% | 100.0% | 100.0% |
| 46 | 61 | 30 | 30 | 1 | 0 | 100.0% | 96.8% | 98.4% |
| 47 | 70 | 35 | 35 | 0 | 0 | 100.0% | 100.0% | 100.0% |
| 48 | 74 | 37 | 37 | 0 | 0 | 100.0% | 100.0% | 100.0% |
| 49 | 70 | 35 | 34 | 2 | 1 | 97.1% | 94.3% | 95.7% |
| 50 | 71 | 35 | 35 | 1 | 0 | 100.0% | 97.2% | 98.6% |
| 51 | 70 | 35 | 35 | 0 | 0 | 100.0% | 100.0% | 100.0% |
| 52 | 86 | 43 | 43 | 1 | 0 | 100.0% | 97.7% | 98.8% |
| 53 | 40 | 20 | 20 | 0 | 0 | 100.0% | 100.0% | 100.0% |
| 54 | 26 | 13 | 13 | 0 | 0 | 100.0% | 100.0% | 100.0% |
| 55 | 57 | 29 | 28 | 1 | 1 | 96.6% | 96.4% | 96.5% |
| 56 | 20 | 10 | 7 | 3 | 3 | 70.0% | 70.0% | 70.0% |
| 57 | 52 | 26 | 24 | 1 | 2 | 92.3% | 96.2% | 94.2% |
| 58 | 44 | 22 | 20 | 3 | 2 | 90.9% | 86.4% | 88.6% |
| 59 | 40 | 20 | 17 | 2 | 3 | 85.0% | 90.0% | 87.5% |
| 60 | 53 | 26 | 26 | 0 | 0 | 100.0% | 100.0% | 100.0% |
| 61 | 42 | 21 | 20 | 0 | 1 | 95.2% | 100.0% | 97.6% |
| 62 | 31 | 15 | 15 | 0 | 0 | 100.0% | 100.0% | 100.0% |
| 63 | 48 | 24 | 24 | 0 | 0 | 100.0% | 100.0% | 100.0% |
| 64 | 39 | 19 | 19 | 0 | 0 | 100.0% | 100.0% | 100.0% |
| 65 | 42 | 21 | 21 | 0 | 0 | 100.0% | 100.0% | 100.0% |
| 66 | 49 | 25 | 22 | 3 | 3 | 88.0% | 87.5% | 87.8% |
| 67 | 43 | 21 | 21 | 0 | 0 | 100.0% | 100.0% | 100.0% |
| 68 | 45 | 22 | 17 | 5 | 5 | 77.3% | 78.3% | 77.8% |
| 69 | 65 | 32 | 27 | 4 | 5 | 84.4% | 87.9% | 86.2% |
| 70 | 53 | 26 | 23 | 2 | 3 | 88.5% | 92.6% | 90.6% |
| 71 | 38 | 19 | 19 | 1 | 0 | 100.0% | 94.7% | 97.4% |
| 72 | 43 | 21 | 17 | 5 | 4 | 81.0% | 77.3% | 79.1% |
| 73 | 44 | 22 | 21 | 1 | 1 | 95.5% | 95.5% | 95.5% |
| 74 | 55 | 27 | 26 | 1 | 1 | 96.3% | 96.4% | 96.4% |
| 75 | 46 | 23 | 22 | 0 | 1 | 95.7% | 100.0% | 97.8% |
| 76 | 43 | 22 | 20 | 0 | 2 | 90.9% | 100.0% | 95.3% |
| 77 | 38 | 19 | 18 | 0 | 1 | 94.7% | 100.0% | 97.4% |
| 78 | 34 | 17 | 17 | 0 | 0 | 100.0% | 100.0% | 100.0% |
| 79 | 52 | 26 | 23 | 2 | 3 | 88.5% | 92.3% | 90.4% |
| 80 | 33 | 17 | 15 | 3 | 2 | 88.2% | 81.3% | 84.8% |
| 81 | 52 | 26 | 26 | 0 | 0 | 100.0% | 100.0% | 100.0% |
| 82 | 44 | 22 | 22 | 0 | 0 | 100.0% | 100.0% | 100.0% |
| 83 | 59 | 29 | 29 | 0 | 0 | 100.0% | 100.0% | 100.0% |
| 84 | 69 | 34 | 34 | 0 | 0 | 100.0% | 100.0% | 100.0% |
| 85 | 55 | 27 | 27 | 0 | 0 | 100.0% | 100.0% | 100.0% |
| 86 | 63 | 31 | 31 | 0 | 0 | 100.0% | 100.0% | 100.0% |
| 87 | 30 | 15 | 15 | 0 | 0 | 100.0% | 100.0% | 100.0% |
| 88 | 46 | 23 | 22 | 1 | 1 | 95.7% | 95.7% | 95.7% |
| 89 | 33 | 17 | 17 | 0 | 0 | 100.0% | 100.0% | 100.0% |
| 90 | 34 | 17 | 15 | 2 | 2 | 88.2% | 88.2% | 88.2% |
| 91 | 42 | 21 | 21 | 0 | 0 | 100.0% | 100.0% | 100.0% |
| 92 | 76 | 37 | 28 | 7 | 9 | 75.7% | 82.1% | 78.9% |
| 93 | 55 | 27 | 26 | 4 | 1 | 96.3% | 85.7% | 90.9% |
| Average | | | | | | 95.5% | 95.6% | 95.6% |

PID=Participant identification number, NOP=total number of phases, NAI=total number
of actual inspirations, TP=number of true positives, FP=number of false positives,
FN=number of false negatives, Sn%=sensitivity, Sp%=specificity, Acc%=accuracy.

It was also of interest to determine whether there was any relationship between the anthropometric measurements and the PI features during inspiration and expiration in any flow level. In this regard, the entire dataset was grouped as shown in Table II, and multivariate analysis of variance (MANOVA) was run for each of the physical parameters. Similar to the ANOVA analysis, this was run separately for the inspiration and expiration. Table V shows the results of this statistical test, with the significant *p*-values highlighted.

**Table V. MANOVA results – Effect of physical parameters on $PI_X$**

**[BMI = Body Mass Index; Exercise = estimated days of cardio exercise per week in last year; Smoking = whether or not the participant was a smoker. d = estimate of dimension of group means; for non-differentiable d = 0; p-values represent the significance of each parameter $PI_i$ in different anthropometric groups.]**

| | $PI_1$ | | $PI_2$ | | $PI_3$ | | $PI_4$ | | $PI_5$ | |
|---|---|---|---|---|---|---|---|---|---|---|
| | Ins. | Exp. | Ins. | Exp. | Ins. | Exp. | Ins. | Exp. | Ins. | Exp. |
| Ethnicity | p = 0.5175 | p = 0.9012 | p = 0.0992 | p = 0.3747 | p = 0.4880 | p = 0.9175 | p = 0.8378 | p = 0.0587 | p = 0.1057 | p = 0.7321 |
| Gender | p = 0.7931 | p = 0.1372 | p = 0.7639 | p = 0.3069 | p = 0.3629 | p = 0.4512 | p = 0.8258 | p = 0.2836 | p = 0.9653 | p = 0.3800 |
| Age | p = 0.4583 0.9899 0.9452 0.8179 | p = 0.1070 0.9343 0.8827 0.7750 | p = 0.4157 0.9545 0.8759 0.9907 | p = 0.9271 0.9096 0.8829 0.8334 | d =1 p = 0.0397 0.2418 0.5335 0.6642 | p = 0.1945 0.6886 0.9560 0.8019 | p = 0.2563 0.7585 0.8001 0.6028 | p = 0.1459 0.3992 0.9376 0.8566 | p = 0.3767 0.9865 0.9638 | p = 0.1245 0.3518 0.8019 |
| Height | p = 0.4078 0.5274 | p = 0.3160 0.6602 | p = 0.6767 0.8563 | p = 0.5089 0.6376 | p = 0.9980 0.9961 | p = 0.8899 0.8273 | p = 0.9072 0.9512 | p = 0.4948 0.6120 | p = 0.1720 0.6798 | p = 0.3707 0.4878 |
| Weight | p = 0.1368 0.8104 0.8226 0.8141 | p = 0.2706 0.4472 0.5281 0.4898 | p = 0.3184 0.5182 0.6644 0.9927 | p = 0.3966 0.7030 0.9912 0.8991 | p = 0.3615 0.8106 0.8961 0.9981 | p = 0.7853 0.9719 0.9865 0.8759 | p = 0.9377 0.9617 0.9920 0.8953 | d =1 p = 0.0379 0.3289 0.4613 0.3993 | p = 0.9470 0.9098 0.9290 | p = 0.1638 0.8103 0.8398 |
| BMI | d =1 p = 0.0037 0.3092 0.2918 | d =2 p = 0.0012 0.0496 0.3575 | p = 0.5990 0.8102 0.8216 | p = 0.1216 0.5887 0.7015 | p = 0.3137 0.5052 0.8495 | p = 0.2335 0.8286 0.8642 | p = 0.5424 0.6256 0.7065 | d =1 p = 0.0001 0.1422 0.2669 | p = 0.0932 0.7437 0.9915 | d =1 p = 0.0000 0.2231 0.2497 |
| Exercise | p = 0.1000 0.6608 0.7014 0.8490 | d =1 p = 0.0176 0.4594 0.6145 0.9124 | p = 0.6779 0.9199 0.9736 0.8906 | d =1 p = 0.0364 0.8095 0.7050 0.5797 | p = 0.1564 0.7447 0.7578 0.6666 | 0.6497 0.7921 0.9156 0.8364 | d =1 p = 0.0217 0.7133 0.7773 0.8116 | p = 0.9472 0.9649 0.9339 0.9874 | d =1 p = 0.0051 0.5305 0.7889 | p = 0.4475 0.6384 0.7107 |
| Smoking | d =1 p = 0.0451 | p = 0.1132 | p = 0.5560 | p = 0.0681 | p = 0.1364 | p = 0.4498 | d =1 p = 0.0233 | p = 0.4381 | p = 0.3185 | p = 0.0800 |

The next statistical test was the paired t-test to determine whether $PI_{1-5}$ showed significant differences between inspiration and expiration phases in the 4 distinct flow levels. A paired t-test was used because the matched inspiration and expiration were part of the same breath cycle. The results are in Table VI with the significant *p*-value and confidence intervals (C.I.) at each flow level.

**Table VI. Paired t-test Result – Effect of flow-level on inspiration/expiration**

**[p-value = strength of null hypothesis testing; C.I. = confidence intervals of inspiration and expiration groups at different flow levels. The highlighted values are significant.]**

|  |  | $PI_1$ | $PI_2$ | $PI_3$ | $PI_4$ | $PI_5$ |
|---|---|---|---|---|---|---|
| Flow level 1 | p-value | 0.65 | 0.002 | 4.78E-16 | 0.0307 | 0.1067 |
| | C.I. | -2.41 ~ 3.84 | -0.65 ~ -0.16 | 90.9 ~ 131.3 | -0.91 ~ -0.005 | -0.136~0.137 |
| Flow level 2 | p-value | 0.89 | 4.25E-04 | 2.75E-14 | 0.004 | 0.0415 |
| | C.I. | -2.50 ~ 2.17 | -1.11 ~ -.33 | 82.1 ~ 123.4 | -0.797~-0.154 | 0.003~0.147 |
| Flow level 3 | p-value | 0.38 | 1.50E-05 | 3.82E-14 | 8.01E-04 | 0.0179 |
| | C.I. | -1.48 ~ 3.86 | -1.50 ~ -0.61 | 96.9 ~ 146 | -0.086~-0.024 | 0.0143~0.146 |
| Flow level 4 | p-value | 0.13 | 3.79E-06 | 1.41E-13 | 0.0024 | 0.02 |
| | C.I. | -0.66 ~ 5.19 | -1.96 ~ -0.86 | 104 ~ 159.7 | -0.095 ~-0.215 | 0.0124~0.158 |

Finally, we ran our phase detection method on the total dataset of 93 subjects using the method described in Eq. (1). The sensitivity and specificity of the phase detection results of the individual and combined PI-parameters on all 93 subjects are shown in Figure 23.
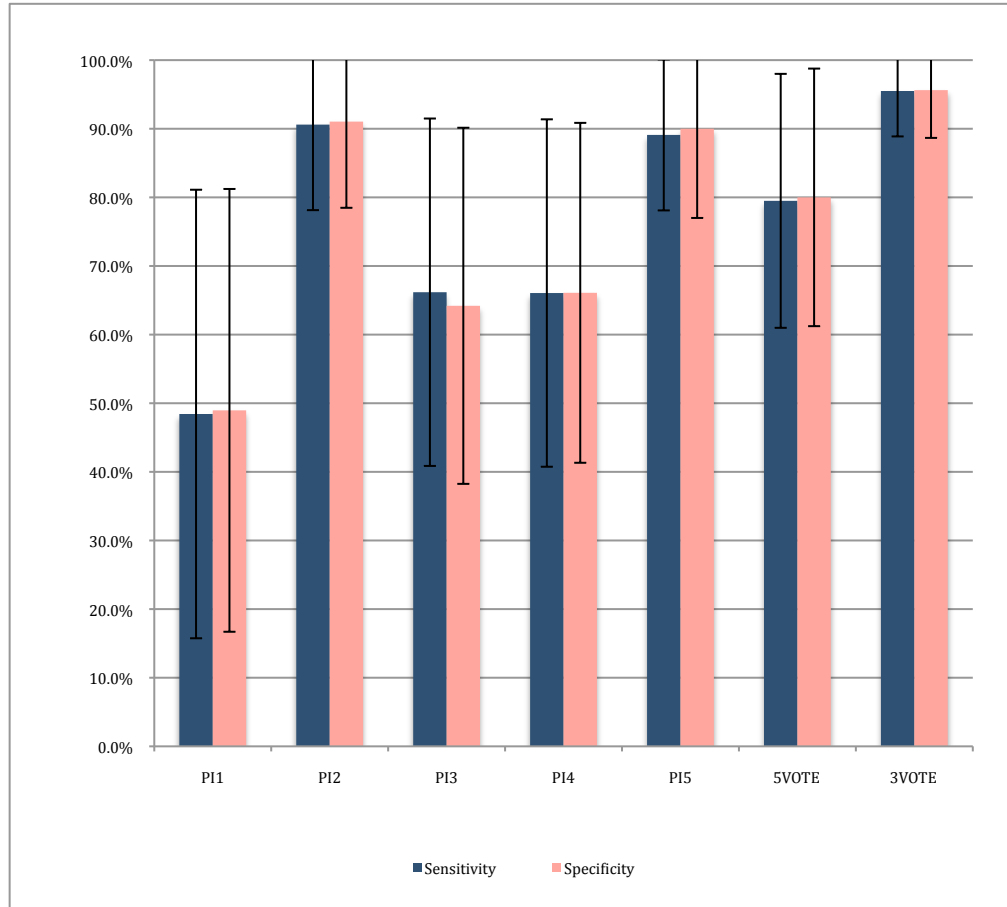
**Figure 23. Overall sensitivity and specificity of the PI and majority-vote indices**

## 4.2    Discussion: Parameter Indices

An interesting observation was made regarding $PI_1$, the intensity parameter of the breath phase. This feature is the most commonly used parameter for the other steps of acoustic flow estimation; however, in terms of phase detection it showed the lowest sensitivity and specificity (Figure 23). This was seen in our preliminary study and corroborated by the findings in this paper.

In comparison to the preliminary study, certain PIs and their combined performances have shown some changes due to a significant change in the data size [**40**]. The quantitative difference between the majority vote methods have significantly

increased as expected, with 3VOTE outperforming the 5VOTE method. Individually $PI_1$ and $PI_5$'s performance has fallen, while $PI_2$ has shown relatively consistent performance. The pseudo-volume parameters, $PI_3$ and $PI_4$'s performances have improved since the preliminary study. The 3VOTE method's sensitivity and specificity have improved to 95.5% and 95.6% respectively. This shows the robust nature of 3VOTE in terms of phase detection.

## 4.3    Statistical Analysis

ANOVA analysis was done in order to understand how the breath phases within the 4 flow levels behaved (Table III). The *p*-values in the first two columns indicate significant changes of the mean values of $PI_1$ and $PI_2$ in relation to flow level in both inspiration and expiration patterns. This suggests that these two parameters could be useful to distinguish *between* flow levels and are not necessarily a good candidate for phase detection. As for $PI_{3-5}$, flow-level variations did not affect these parameters. This was expected as $PI_{3,4}$ are pseudo-volume measures and $PI_5$ is a gradient measure that will not change greatly with changes in flow level. This makes these parameters more robust choices for phase detection over long breath recordings where the flow level is often variable.

Table V shows the statistical results between the physical measurements (age, height, weight, chest diameter, waist diameter, neck diameter, body mass index, percentage body fat and days of exercise per week) and the phase indices. Out of the measured anthropometric parameters, ethnicity, gender and height showed no significance, while weight, BMI, exercise and smoking history showed significant impact on the phase parameters extracted from both inspiratory and expiratory patterns.

One can speculate that this alludes to the fact that inspiration is an active process and expiration is a passive process. Since active processes are controlled by neural impulses, they are not as dependent on physical parameters or activity (e.g. weight, exercise, smoking history, etc). On the other hand, the passive process of expiration that uses the natural recoiling of the lung tissues has more relationship with smoking history, weight and BMI. This suggests that physical attributes and habits affect the expiratory cycle of breathing.

In order to better understand the relationships of the PI-parameters and the actual breath phases, paired t-tests were run (Table VI). It was interesting to note that all except the intensity-parameter, $PI_1$, showed statistically significant difference between inspiration and expiration phases in each of the 4 flow levels. The highlighted *p*-values in Table VI show strong significance to reject the null hypothesis and indicate that the indices $PI_{2-5}$, show differences in mean value in the four flow levels between inspiration and expiration. This supports the idea of using these parameters for phase detection.

It was difficult to determine which of the two pseudo-volume parameters, $PI_{3,4}$, to include in the 3VOTE phase detection method. Since their sensitivity and specificities were similar, it was evident that they carried the same information in terms of phase-detection. The relationship of $PI_3$ with physical parameters was the determining factor. By choosing to exclude $PI_3$ from the voting-algorithm, we hoped to exclude any variation in the performance of the program due to differences in body type.

It was understood from the beginning of this study that we would be looking at healthy participants/volunteers' breathing patterns and that the findings of this study would be the basis of proving the concept of the 3VOTE method before taking it further

to study patient data. As a result, addressing how this algorithm would perform on patient data was beyond the scope of this project. Nevertheless, we have hypothesized plausible scenarios for patient data in Appendix A and discussed in detail how 3VOTE would perform on the synthesized scenarios.

# CHAPTER V

# CONCLUSION AND FUTURE WORK

## 5.1 Conclusions

This study sought to develop a robust phase detection method using only tracheal breath sounds without assuming the breath phase alternation. Previous studies required a secondary channel (lung sounds) to determine the subject's breath phase or simply assumed breath phases to be alternating. Other studies that were focused more on flow-estimation, still required airflow for calibration purposes. The method developed in this study overcomes these previous limitations, uses only tracheal breath sound, and is designed to identify breath phases even in case of swallowing or apnea episodes where the regular breathing pattern is perturbed. Strict guidelines were set for dataset development and recording protocols were followed for healthy participants' flow and tracheal sound recordings. The results of the proposed method show a very high accuracy of correctly determining breath phase (95.6% with sensitivity: 95.5%, specificity: 95.6%) for all different flow rates.

## 5.2 Future Direction

In another study it was seen that tracheal sounds have some significant frequency components below 300Hz [38]. A heart sound cancellation method was used to reduce the effects of heart sound interference and tracheal sound signals were low-pass filtered instead of band-pass filtering [51]. Although we did not apply this to our method, we

speculate that by including more characteristic features of tracheal breath sounds and by reducing the effects of heart sounds, our method of phase detection will improve even further, especially in the shallow flow rates.

We chose to use LV as the primary feature to extract the phase-index-parameters. This was based on the results of [**40**] where LV had outperformed average-power, within the frequency range 150-800 Hz, in differentiating between breath phases. However, other energy features such as average-power, or entropy of a signal, can also be used and the PI-parameters can be extracted from them. The key step is proper onset detection so that a recording can be segmented into a chain of consecutive breath phases.

The phase detection method developed here only needs 3 consecutive breath phases in order to determine the class of the central breath phase. There is no training necessary for this system; it is also independent of the subject's fitness or body type. It has been applied to a wide range of healthy participants, from underweight to obese, from teenagers to seniors and has shown very high accuracies all throughout.

One of the major obstacles with respiratory acoustics is the challenge of variable flow levels; most models designed in literature are confined to a specific flow level, and often avoid shallow breathing altogether. The method developed here was applied to 4 flow levels, including shallow breathing (FL1: 0~7.5mL/s/kg) and showed consistent results. This is very advantageous, especially in long night recordings where the patients often breathe in shallow and low flow levels.

Having stated the advantages of the proposed phase detection method, we acknowledge that it has only been applied to healthy subjects' data during wakefulness. Thus its ability to perform phase detection with the same accuracy with patients' data is

an area that is unexplored. Regardless, we have discussed in detail how we interpret this method performing with various hypothetical scenarios in Appendix A. The results of this study are promising and should be researched further, especially during sleep and/or swallowing assessment.

# APPENDIX A

# 3VOTE METHOD AND PLAUSIBLE SCENARIOS

There are a few plausible scenarios for breathing such as normal breathing in which the breath phases simply alternates but the duration of breaths may change, breathing with a deglutition apnea for occasional swallowing (in a breathing assessment), breathing with sleep apnea, or successive inspiration/expiration. The normal alternating phases is the most common pattern of breathing; however, other breathing patterns also do occur. How our developed voting method would handle phase identification, are being described by the following synthesized examples from Figure 24 to Figure 28.

## A.1   Scenario 1: Alternate Breathing with Varied Durations

The Fig.A.1 below shows a schematic diagram of a flow signal for regular breathing with 'time' as the x-axis. If we consider the two breath phases for any given respiratory cycle, we notice certain traits that exist for each of the 5 PIx's. Let's focus on one inspiration phase (c) shown in Fig.A.1. The duration of expirations are normally longer than inspiration; therefore the PI2-vote(n)<0 indicating an inspiration. For regular breathing the PI4, over the expiration phase yields a higher value; thusPI4-vote(n)<0 indicating an inspiration. The gradient of an inspiratory phase is higher than that of an expiratory phase. Thus, PI5-vote(n)>0 is indicative of an inspiration.

Thus the majority of the 3VOTE method yields 'c' as an inspiration phase.
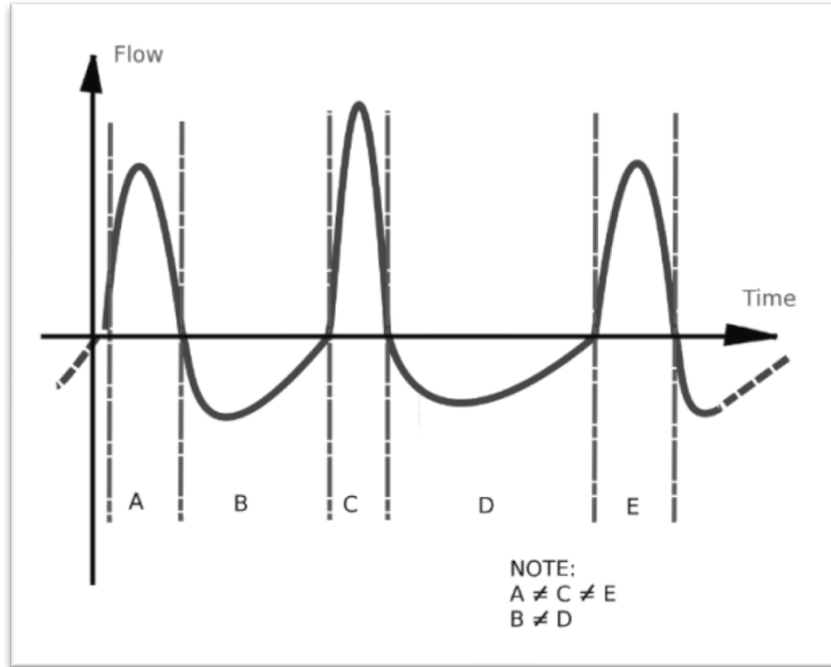
**Figure 24. Synthesized scenario 1: Alternate breathing with varied durations**

## A.2   Scenario 2: Non-Breath Event in Regular Breathing

In such a situation, the onset detection method will ignore the swallowing phase as it will detect it as noise. Since the noise segment will not be considered as a phase, essentially, the algorithm will see no difference between scenario 1 and scenario 2.
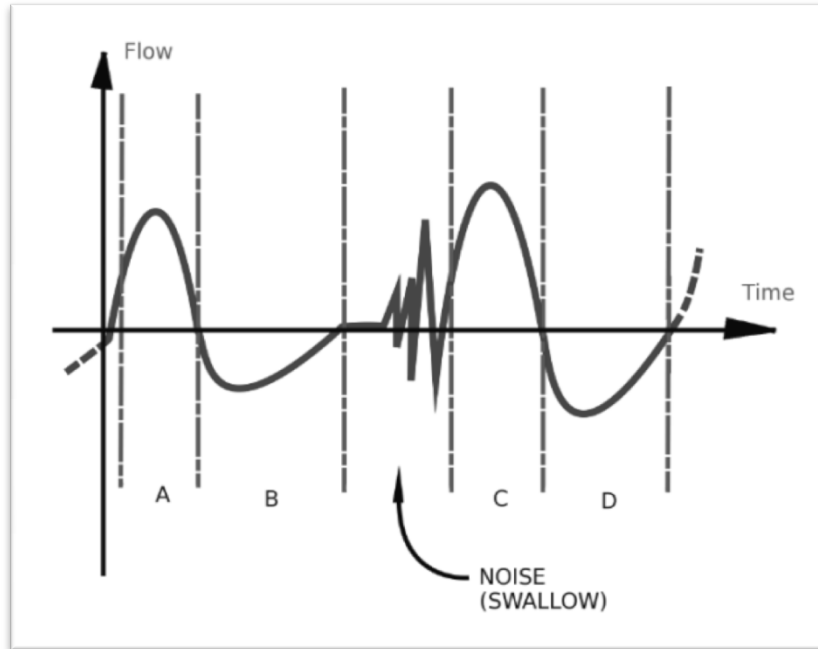


**Figure 25. Synthesized scenario 2: Non-breath event & regular breathing**

**(-ins-exp-noise-ins-exp)**

## A.3   Scenario 3: Non-Breath Event, Irregular Breathing

In such a case that a swallowing (or noise) occur between two expirations (a common pattern of swallowing in children), the difficulty would be to determine the phases for 'b' and 'c'.
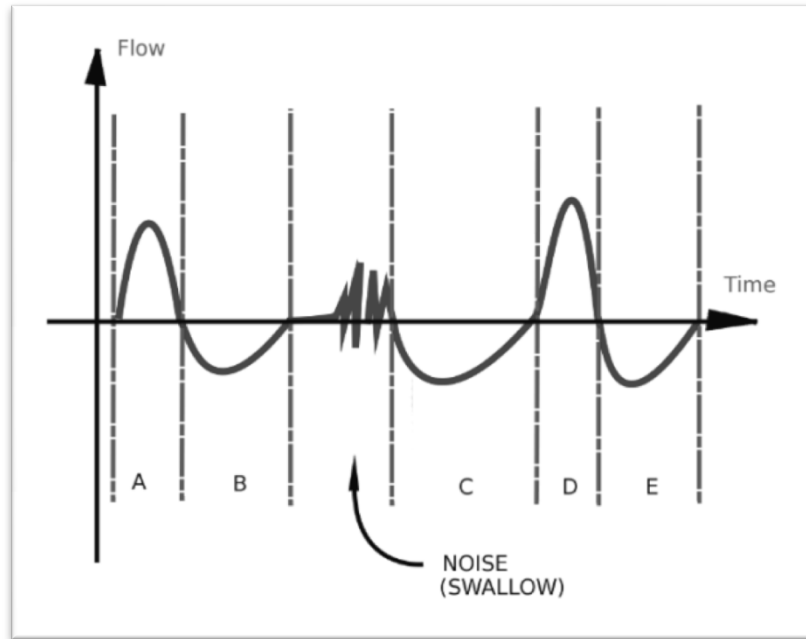


**Figure 26. Synthesized scenario 3: Non-breath event, irregular breathing**

**(-ins-exp-noise-exp-ins-exp-)**

Using the 3VOTE method, for phase 'b' =n, we will have:

PI12>0, PI22≈0*  → PI2-vote(b)>0 => expiration

PI14>0, PI24≈0*  → PI4-vote(b)>0 => expiration

PI15<0, PI25≈0*  → PI5-vote(b)<0 => expiration

For phase 'c' = n:

PI12≈0*, PI22>0  → PI2-vote(c)>0 => expiration

PI14≈0*, PI24>0  → PI4-vote(c)>0 => expiration

PI15≈0*, PI25<0  → PI5-vote(c)<0 => expiration

66

Therefore, the 3VOTE method still yields correct phase identification.

*Regardless of the sign of these values, they will be very close to zero, causing the PIx-

vote(n) to rely more on the alternate comparison.

## A.4   Scenario 4: Non-Breath Event, Irregular Breathing
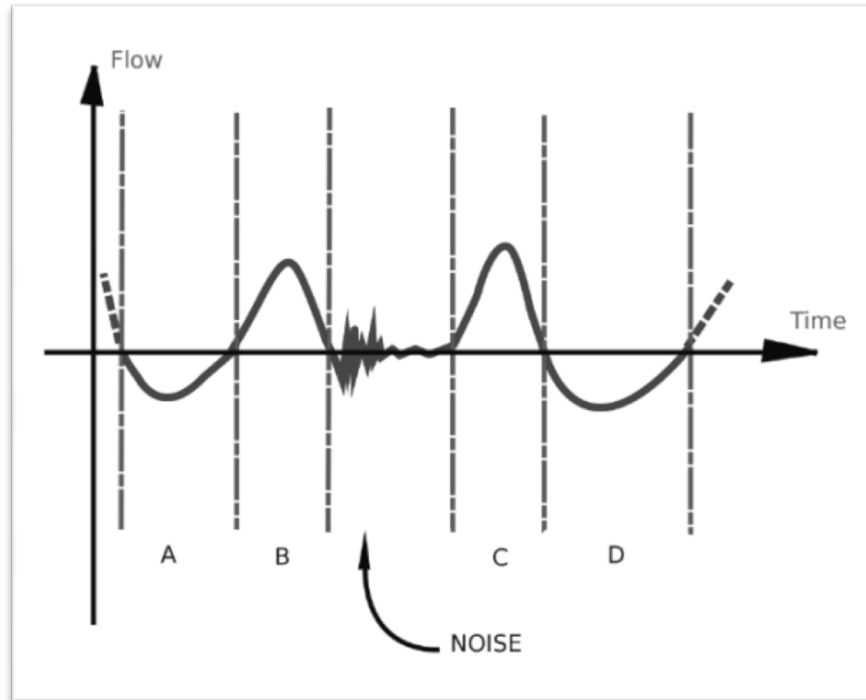


**Figure 27. Non-breath event, irregular breathing**

**(-exp-ins-noise-ins-exp-)**

Similar to scenario 3, to determine the phases for 'b' and 'c' segments, using the

3VOTE method we will have:

PI12<0, PI22≈0*  → PI2-vote(b)<0 => inspiration

PI14<0, PI24≈0*  → PI4-vote(b)<0 => inspiration

PI15>0, PI25≈0*  → PI5-vote(b)>0 => inspiration

For phase 'c' = n:

PI12≈0*, PI22<0  → PI2-vote(c)<0 => inspiration

PI14≈0*, PI24<0  → PI4-vote(c)<0 => inspiration

PI15≈0*, PI25>0  → PI5-vote(c)>0 => inspiration

## A.5  Scenario 5: Successive Inhalation or Exhalation
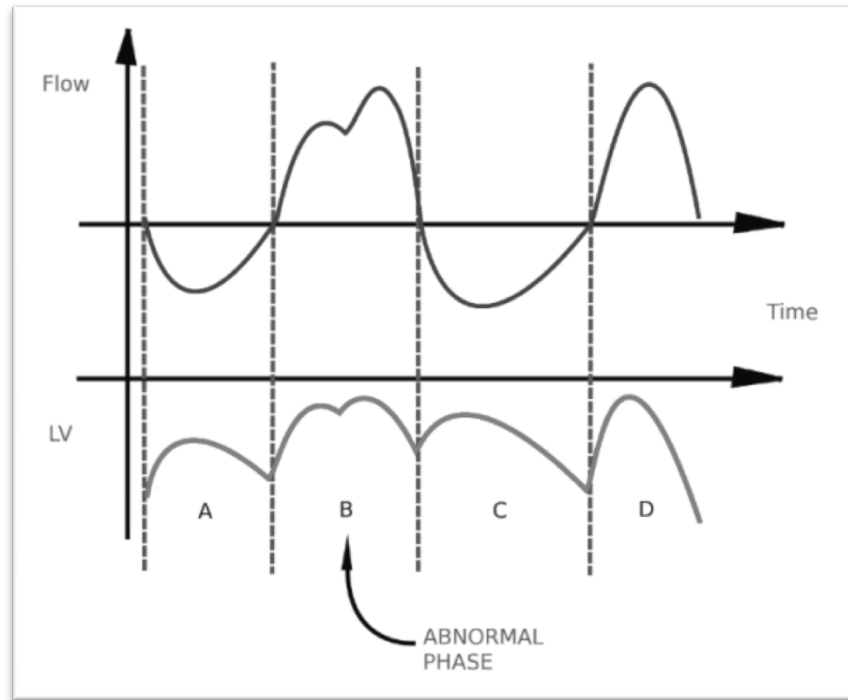


**Figure 28. Synthesized scenario - successive inhalations/exhalations**

**(-exp-ins-ins-exp)**

The above pattern is rare but it may occur especially in children. In such situations, the onset detection method overlooks the local minima, and considers 'b' as a single breath phase. That is because in the LV signal, the local minima will be less than half the drop from the maxima and first onset of the breath phase. Thus, the algorithm will not consider the phase complete until it reaches the next minima. In such cases, the duration (PI2) index may indicate the wrong phase; however, the volume and gradient indices (PI4, PI5) will still correctly identify the breath phases. Thus using the majority-vote will still yield the correct phase detection.

# APPENDIX B

# COPYRIGHT AND PERMISSIONS FOR IMAGES

There are a total of 34 tables, diagrams, schematics and pictures displayed throughout this manuscript. I have created the majority of these figures (as well as the tables) specifically for this manuscript as products of my analysis and visual aids for this document. Matlab (version 7.9), Microsoft excel (version 12.3 for mac) and GIMP (image processing software, version 2.6) were used for the figures and tables I mention here. In particular, these are figures 5, 9, 10 through to 28, as well as tables I through to VI.

The remaining figures were either from the public domain or permission was sought to use them in this manuscript. Figures 1 and 3 were from the webster's online dictionary which is a public domain site. The permissions for the remainder of the figures are as follows:

For figures 2, 4, 7 and 8:

E-mail: nhlbiinfo@nhlbi.nih.gov
Web site: http://www.nhlbi.nih.gov

------------------ Original Message ------------------
From: Huq, Saif
Received: 12/4/2011 5:51 PM
To: Information Center, NHLBI; NHLBI Health Information Center
Subject: Copyright permission request for attached image - polysomnography image

SUBJECT LINE: Copyright permission request for ARTICLE/GRAPH/IMAGE/OTHER

DATE: December 4th, 2011

Attention: Permissions Manager

I am requesting permission to include in my graduate THESIS/DISSERTATION/PRACTICUM the image from the following url:

1.  http://www.nhlbi.nih.gov/health/health-topics/topics/slpst/

My thesis, entitled "Automatic Breath Phase Detection using only Tracheal Breath Sounds", is part of the requirements needed to graduate from the Faculty of Graduate Studies at the University of Manitoba.

My thesis will be available in paper format from the University of Manitoba Libraries. It will also be posted electronically and will be accessible for free to a worldwide audience from the University of Manitoba's digital repository called MSpace located at http://mspace.lib.umanitoba.ca/index.jsp and from Library and Archives Canada's Theses Portal located at http://www.collectionscanada.gc.ca/thesescanada/index-e.html

**I do not expect any commercial profits from my thesis.**

Please reply to confirm if you are the copyright owner of the works and **if permission is granted to include them in my master's degree manuscript**. If you do not control the copyright on the above-mentioned works, I would appreciate any contact information you can provide regarding the proper rights holder.

Thank you.

Saiful Huq, M.Sc. in Eletrical Engineering
Dept. of Electrical and Computer Engineering, Faculty of Engineering
1-204-995-7243
<saifulhuq@gmail.com>

--
Kind regards,
Saif

For figure 6:

**7-spirometry.jpg**
115K

---

**daviddarling@daviddarling.info <daviddarling@daviddarling.info>**       **Mon, Dec 5, 2011 at 12:13 AM**
To: Saif Huq <saifulhuq@gmail.com>

Dear Saif,

You are welcome to use the requested image in your thesis.

Best regards,
David Darling

> SUBJECT LINE: Copyright permission request for ARTICLE/GRAPH/IMAGE/OTHER
>
> DATE: December 4th, 2011
>
>
> Attention: Permissions Manager
>
>
>
> I am requesting permission to include in my graduate
> THESIS/DISSERTATION/PRACTICUM the image from the following url:
>
>
>
> 1. http://www.daviddarling.info/encyclopedia/S/spirometry.html
>
> My thesis, entitled "Automatic Breath Phase Detection using only Tracheal
> Breath Sounds", is part of the requirements needed to graduate from the
> Faculty of Graduate Studies at the University of Manitoba.
>
>
>
> My thesis will be available in paper format from the University of
> Manitoba
> Libraries. It will also be posted electronically and will be accessible
> for free to a worldwide audience from the University of Manitoba's digital
> repository called MSpace located
> athttp://mspace.lib.umanitoba.ca/index.jsp and
> from Library and Archives Canada's Theses Portal located at
> http://www.collectionscanada.gc.ca/thesescanada/index-e.html
>
>

>
> *I do not expect any commercial profits from my thesis. *
>
>
>
> Please reply to confirm if you are the copyright owner of the works and*
> if
> permission is granted to include them in my master's degree manuscript*.
> If
> you do not control the copyright on the above-mentioned works, I would
> appreciate any contact information you can provide regarding the proper
> rights holder.
>
>
>
> Thank you.
>
>
>
> Saiful Huq, M.Sc. in Eletrical Engineering
>
> Dept. of Electrical and Computer Engineering, Faculty of Engineering
>
> 1-204-995-7243
begin_of_the_skype_highlighting                    1-204-995-7243        end_of_the_skype_highlighting
[Quoted text hidden]

# REFERENCES

[1] V Mckusick MD, "Cardiovascular sound in health and disease," *American Journal of Medical Sciences*, vol. 238, no. 1, p. 128, 1959.

[2] M Younes, "Contributions of upper airway mechanics and control mechanics and control mechanisms to severity of obstructive apnea," *American thoracic society*, 2003.

[3] J Fiz et al., "Acoustic analysis of vowel emission in obstructive sleep apnea," *CHEST*, vol. 104, no. 4, pp. 1093-1096, 1993.

[4] M Mussell and Y Miyamoto, "Comparison of normal respiratory sounds recorded from the chest and trachea at various respiratory air flow levels," *Frontiers of medical biology and engineering*, vol. 4, no. 2, pp. 73-85, 1992.

[5] H Pasterkamp, S Kraman, and G Wodicka, "Respiratory Sounds: Advances beyond the stethoscope," *American journal of respiratory and critical care medicine*, vol. 156, no. 3, pp. 974-976, 1997.

[6] J Bullock, J Boyle, and M Wang, *Nathonal Medical Series for Independent Study: Physiology 4th Edition*.: Lippincott Williams & Wilkins, 2001.

[7] Thomas J Prendergast and Stephen J Ruoss, *McPhee SJ, Ganong WF: Pathophysiology of Disease 5th Editino*".: McGraw-Hill, 2009.

[8] J Chuah and Z Moussavi, "Automated Respiratory Phase Detection by Acoustical Means," in *Systems, Cybernetics & Informatics*, 2000, pp. 228-231.

[9] I Hossein and Z Moussavi, "Respiratory airflow estimation by acoustical means," in *IEEE EMBS*, 2002.

[10] D Paydarfar, R Gilbert, C Poppel, and P Nassab, "Respiratory phase resetting and airflow changes induced by swallowing in humans," *Journal of Physiology*, vol. 483, pp. 273-288, 1995.

[11] N Cherniack and J Widdicombe, *Handbook of Physiology*.: Oxford Printing press, 1986, vol. II.

[12] W. Dorland MD, *Dorland's Medical Dictionary*.: Elsevier Publications, 2007.

[13] RG Breeze and EG Wheeldon, "The cells of the pulmonary airways," *American Review of Respiratory Disease*, pp. 116-705, 1977.

[14] LC Junqueira and J Carneiro, *Basic Histology: Text and Atlas, 11th Edition*.: McGraw-Hill, 2005.

[15] Webster's Online Dictionary. (2011, Dec.) "Webster's Online Dictionary" - Definition: Respiratory System. [Online]. HYPERLINK "http://www.websters-online-dictionary.org/definitions/Respiratory%20System" http://www.websters-online-dictionary.org/definitions/Respiratory%20System

[16] C Jolley and J Moxham, "Respiratory Muscles, Chest Wall, Diaphragm, and Other," *European Respiratory Journal*, vol. 32, pp. 632-643, 2006.

[17] National Heart Lung and Blood Institute People Science Health. (2011, Dec.) What is Primary Ciliary Dyskinesia. [Online]. HYPERLINK "http://www.nhlbi.nih.gov/health/health-topics/topics/pcd/printall-index.html" http://www.nhlbi.nih.gov/health/health-topics/topics/pcd/printall-index.html

[18] Shifren and Adrian, *The Washington Manual: Pulmonary Medicine Subspecialty Consult, 1st Edition*.: Lippincott Williams & Wilkins, 2006.

[19] MG Levitzky, *Pulmonary Physiology 5th Ed*. New York: McGraw-Hill, 1999.

[20] National Heart Lung and Blood Institute People Science Health. (2011, Dec.) The Respiratory System. [Online]. HYPERLINK "http://www.nhlbi.nih.gov/health/health-topics/topics/hlw/system.html" http://www.nhlbi.nih.gov/health/health-topics/topics/hlw/system.html

[21] J Seikel, D King, and D Drumright, *Anatomy & Physiology for Speech, Language and Hearing*.: Thomas Delmar Learning, 2005.

[22] T Isono, E Hajduk, R Brant, W Whitelaw, and J Remmers, "Interaction of cross-sectional area, driving pressure and airflow of passive velopharynx," *Applied Physiology*, vol. 83, no. 3, p. 851, 1997.

[23] R Gilbert, J Auchincloss, J Brodsky, and W Boden, "Changes in tidal volume, frequency, and ventilation induced by their measurement," *Journal of Applied Physiology*, vol. 33, no. 2, pp. 252-254, 1972.

[24] NR Anthonisen and RM Cherniack, *Ventilatory Control in lung disease*. New York: Marcel Dekkar Inc, 1981.

[25] G Tortora and S Reynolds, *Principles of Anatomy and Physiology*. Hoboken, NJ: John Wiley & Sons Inc., 2001.

[26] GF Alheid, WK Milsom, and DR McCrimmon, "Pontine influences on breathing: an overview," *Resp. Physiology and Neurobiology*, vol. 143, pp. 105-114, 2004.

[27] J Duffin, K Ezure, and J Lipski, "Breathing Rhythm Generation: Focus on Rostral Ventrolateral Medulla," *News in Physiological Sciences*, vol. 10, pp. 133-140, 1995.

[28] K EZURE, "Synaptic connections between medullary respiratory neurons and considerations on the genesis of respiratory rhythm," *Progress in neurobiology*, vol. 35, pp. 429-450, 1990.

[29] M Abella, J Formolo, and D Penney, "Comparison of the acoustic properties of six popular stethoscopes," *Journal of the acoustic society of america*, vol. 91, p. 2224, 1992.

[30] F Yen, K Behbehani, E Lucas, J Burk, and J Axe, "A noninvasive technique for detecting obstructive and central sleep apnea," in *IEEE EMBS*, vol. 44, 2002.

[31] P Enright, L Johnson, J Connett, H Voelker, and A Buist, "Spirometry in the Lung Health Study. 1. Methods and quality control.," *Am Rev Respir Dis.*, vol. 143, pp. 1215-23, 1991.

[32] R Pellegrino et al., "Interpretative Strategies for Lung Function Tests," *Eur Respir J*, no. 26, pp. 948-968, 2005.

[33] N Pride, "The assessment of airflow obstruction: Role of measurements of airways

resistance and of tests of forced expiration," *British Journal of Diseases of the Chest*, vol. 65, pp. 135-169, 1971.

[34] D Darling. The Encyclopedia of Science. [Online]. HYPERLINK "http://www.daviddarling.info/encyclopedia/S/spirometry.html" http://www.daviddarling.info/encyclopedia/S/spirometry.html

[35] National Heart Lung and Blood Institute People Science Health. (2011, Dec.) What to Expect During a Sleep Study. [Online]. HYPERLINK "http://www.nhlbi.nih.gov/health/health-topics/topics/slpst/during.html" http://www.nhlbi.nih.gov/health/health-topics/topics/slpst/during.html

[36] National Heart Lung and Blood Institute People Science Health. (2011, Dec.) What is Oxygen Therapy? [Online]. HYPERLINK "http://www.nhlbi.nih.gov/health/health-topics/topics/oxt/printall-index.html" http://www.nhlbi.nih.gov/health/health-topics/topics/oxt/printall-index.html

[37] J Ashkanazi, P Silverberg, R Foster, a Hyman, and j milic-emili, "Effects of respiratory apparatus on breathing pattern," *Journal of applied physiology*, vol. 48, pp. 577-580, 1980.

[38] Z Moussavi, "Fundamentals of respiratory sounds and analysis," Lectures on Biomedical Engineering, University of Manitoba, 2006.

[39] A Yadollahi and Z Moussavi, "Measuring Minimum Critical Flow for Normal Breath Sounds," in *IEEE EMBS*, 2005.

[40] S Huq and Z Moussavi, "Automatic Breath Phase Detection using only Tracheal Sounds," in *IEEE EMBS*, 2010, pp. 272-275.

[41] Z Moussavi, M Leopando, H Pasterkamp, and G Pempel, "Computerized acoustical respiratory phase detection without airflow measurement," *Inst. Elect. Engg. Journal Med. Biology Engg. Comp.*, vol. 38, no. 2, pp. 198-203, 2000.

[42] C Weissman, J Ashkanazi, J Milic-Emili, and J Kinney, "Effect of respiratory apparatus on respiration," *Journal of Applied Physiology*, vol. 57, pp. 457-480, 1984.

[43] J Earis and B Cheetham, "Future perspectives for respiratory sound research," *European respirator review*, vol. 10, no. 77, pp. 641-646, 2000.

[44] G Souffet et al., "Interaction between tracheal sounds and flow rate: a comparison of some different flow evaluations from lung sounds," *IEEE Trans. Biomed. Engg.*, vol. 37, no. 4, pp. 384-391, 1990.

[45] R. K. Moore A. P. Varga, "Hidden Markov Model Decomposition of Speech and Noise," in *bcc*, 1990.

[46] A Yadollahi and Z Moussavi, "Formant analysis of breath and snore sounds," *EMBS*, p. 2563, 2009.

[47] M Katz, "Fractals and the analysis of waveforms," *Comput. Biol. Med.*, vol. 18, no. 3, pp. 145-156, 1998.

[48] D Joanes and C Gill, "Comparing measures of sample skewness and kurtosis," *Journal of the Royal Statistical Society: Series D (The Statistician)*, vol. 47, no. 1,

pp. 183-189, 1998.

[49] P Várady, T Micsik, S Benedek, and Z Benyó, "A novel method for the detection of apnea and hypopnea events in respiration signals," in *IEEE Biomedical Engg.*, vol. 49, 2002.

[50] A Yadollahi and Z Moussavi, "A Robust Method for Estimating Respiratory Flow Using Tracheal Sound Entropy," *IEEE EMBS*, vol. 53, no. 4, p. 2006.

[51] A Yadollahi and Z Moussavi, "A Robust Method for Heart Sound Localization using Lung Sounds Entropy," *IEEE Trans. Biomed. Engg.*, vol. 53, no. 3, pp. 497-502, 2006.

[52] V Iyer, P Ramamorthy, H Fan, and Y Ploysongsang, "Reduction of heart sounds from respiratory sounds by adaptive filltering," *IEEE Trans. Biomed. Engg.*, vol. 33, no. 12, pp. 1141-1148, 1986.

[53] N Gavriely and D Cugell, "Airflow effects on amplitude and spectral content of normal breath sounds," *Journal of Applied Physiology*, vol. 80, pp. 5-13, 1996.

[54] A Sovijarvi et al., "characteristic of breath sounds and adventitious respiratory sounds," *Eur. Resp. Rev.*, pp. 591-596, 2000.

[55] M Kompis and E Russi, "Adaptive heart-noise reduction of respiratory sounds recorded by a single microphone," in *14th Ann. Int. Conf. IEEE EMBS*, 1992, pp. 691-692.

[56] A Yadollahi and Z Moussavi, "Comparison of flow-sound relationship for different features of tracheal sound," *EMBS*, p. 805, 2008.

[57] M Golabbakhsh, "Tracheal breath sound relationship with respiratory flow: modeling, the effect of age and airflow estimation," Elec. & Comp. Engg., University of Manitoba, 2004.

[58] Y Yap and Z Moussavi, "Acoustical Airflow Estimation From Tracheal Sound Power," in *Canadian Conf. Elec. Comp. Engg.*, 2002, pp. 1073-76.

[59] S Huq and Z Moussavi, "Breath Analysis of Respiratory Flow using Tracheal Sounds," in *IEEE ISSPIT*, 2007, pp. 414-418.

[60] A Yadollahi and Z Moussavi, "The Effect of Anthropometric Variations on Acoustical Flow Estimation: Proposing a Novel Approach for Flow Estimation Without the Need for Individual Calibration," *IEEE Biomed. Engg.*, vol. 58, no. 6, p. 1663, 2011.

[61] RM Cherniack and MB Raber, "Normal standards for ventilatory function using an automated wedge spirometer," *The American Review of Respiratory Disease*, vol. 106, no. 1, pp. 38-46, 1972.

[62] J Proakis and D Manolakis, *Digital signal processing: principles, algorithms, and applications*. Upper Saddle River, NJ: Prentice Hall, 1996.

[63] R Hogg and J Ledolter, *Engineering statistics.*: Macmillan Publ. Comp, 1989.